Free Radical Biology and Medicine 191 (2022) 176–190

Contents lists available at ScienceDirect

Free Radical Biology and Medicine

journal homepage: www.elsevier.com/locate/freeradbiomed

LONP1 downregulation with ageing contributes to osteoarthritis via mitochondrial dysfunction

Yuzhe He [a,b,c,1], Qianhai Ding [a,b,c,1], Wenliang Chen [a,b,c,1], Changjian Lin [a,b,c], Lujie Ge [a,b,c], Chenting Ying [a,b,c], Kai Xu [a,b,c], Zhipeng Wu [d], Langhai Xu [e], Jisheng Ran [a,b,c], Weiping Chen [a,b,c,**], Lidong Wu [a,b,c,*]

[a] Department of Orthopedic Surgery, The Second Affiliated Hospital, Zhejiang University School of Medicine, Hangzhou City, Zhejiang Province, China
[b] Orthopedics Research Institute of Zhejiang University, Hangzhou City, Zhejiang Province, PR China
[c] Key Laboratory of Motor System Disease Research and Precision Therapy of Zhejiang Province, Hangzhou City, Zhejiang Province, PR China
[d] Department of Orthopaedics, The First Affiliated Hospital of Zhejiang Chinese Medical University, Hangzhou, Zhejiang Province, China
[e] Department of Pain, Zhejiang Provincial People's Hospital, People's Hospital of Hangzhou Medical College, Hangzhou, China

ARTICLE INFO

Keywords:
Osteoarthritis
LONP1
Mitochondria
Ageing

ABSTRACT

Osteoarthritis (OA) is an age-related disorder and an important cause of disability that is characterized by a senescence-associated secretory phenotype and matrix degradation leading to a gradual loss of articular cartilage integrity. Mitochondria, as widespread organelles, are involved in regulation of complex biological processes such as energy synthesis and cell metabolism, which also have bidirectional communication with the nucleus to help maintain cellular homeostasis and regulate adaptation to a broad range of stressors. In light of the evidence that OA is strongly associated with mitochondrial dysfunction. In addition, mitochondria are considered to be the culprits of cell senescence, and mitochondrial function changes during ageing are considered to have a controlling role in cell fate. Mitochondrial dysfunction is also observed in age-related OA, however, the internal mechanism by which mitochondrial function changes with ageing to lead to the development of OA has not been elucidated. In this study, we found that the expression of Lon protease 1 (LONP1), a mitochondrial protease, was decreased in human OA cartilage and in ageing rat chondrocytes. Furthermore, LONP1 knockdown accelerated the progression and severity of osteoarthritis, which was associated with aspects of mitochondrial dysfunction including oxidative stress, metabolic changes and mitophagy, leading to downstream MAPK pathway activation. Antioxidant therapy with resveratrol suppressed oxidative stress and MAPK pathway activation induced by LONP1 knockdown to mitigate OA progression. Therefore, our findings demonstrate that LONP1 is a central regulator of mitochondrial function in chondrocytes and reveal that downregulation of LONP1 with ageing contributes to osteoarthritis.

1. Introduction

Osteoarthritis (OA) is a very common degenerative disease with high morbidity and disability that is characterized by cartilage extracellular matrix (ECM) degradation, synovial inflammation, osteophyte formation, subchondral bone remodelling and subsequent joint failure [1,2]. The aetiology of OA is multifactorial and includes factors such as age, trauma, obesity, stress, and congenital joint deformities [3,4]. OA is a typical representative of age-related diseases [1]; according to statistics, it affects 14% of people over the age of 60 [5]. Although the relationship between ageing and OA is incompletely understood [6], some recent studies have indicated that cellular senescence is a contributor to age-related loss of function in musculoskeletal diseases, including joint diseases [7]. Chondrocytes, the only cell type in mature cartilage, maintain the structure and function of cartilage and change

* Corresponding author. Department of Orthopedic Surgery, the Second Affiliated Hospital, Zhejiang University School of Medicine, Hangzhou City, Zhejiang Province, China.
** Corresponding author. Department of Orthopedic Surgery, the Second Affiliated Hospital, Zhejiang University School of Medicine, Hangzhou City, Zhejiang Province, China.
E-mail addresses: ze_cwp@zju.edu.cn (W. Chen), wulidong@zju.edu.cn (L. Wu).
[1] These three authors contributed equally to this work.

https://doi.org/10.1016/j.freeradbiomed.2022.08.038
Received 19 July 2022; Received in revised form 18 August 2022; Accepted 29 August 2022
Available online 3 September 2022

Abbreviations

OA	Osteoarthritis
ECM	extracellular matrix
ROS	reactive oxygen species
MMPs	matrix metalloproteinases
LONP1	Lon protease 1
MQC	mitochondrial protein quality control
DEGs	differentially expressed genes
OCR	oxygen consumption rate
DMM	destabilization of the medial meniscus
Res	resveratrol
Tb.Th	trabecular thickness
BV/TV	bone volume fraction
Tb.Sp	trabecular separation
micro-CT	microcomputed tomography
Δψ	Mitochondrial membrane potential
SA-β-gal	Senescence-associated β-galactosidase
UPRmt	mitochondrial unfolded protein response
ISR	integrated stress response

pathologically when OA occurs [8]. Some physicochemical stimuli, such as abnormal mechanical loading or proinflammatory cytokines, can damage chondrocytes and induce inflammatory responses, which accelerate the progression of OA.

Mitochondria are multifunctional organelles that not only produce ATP but also play a role as the main regulatory centres to coordinate vital physiological processes, including apoptosis, macromolecular synthesis, immune response, calcium regulation and intracellular signalling [9–11]. An increasing number of studies have shown that mitochondrial dysfunction is an important factor in the development and progression of OA [12]. Mitochondrial dysfunction in chondrocytes can increase the production of reactive oxygen species (ROS), reduce the synthesis of ATP and induce the synthesis of matrix metalloproteinases (MMPs). Mitochondrial DNA mutations lead to functional differences between subgroups of patients that make patients susceptible to OA [13]. Reducing mtDNA damage can maintain mitochondrial function and chondrocyte homeostasis [14]. In addition, ROS levels in cartilage increase with age, and older chondrocytes are more susceptible to ROS-mediated cellular senescence [15,16]. Significant changes in mitochondrial morphology and function occur in senescent cells, and mitochondrial dysfunction has been considered a culprit of cellular senescence [7,17,18], suggesting that mitochondria can be a therapeutic target for antiaging treatments to reduce the incidence of OA in elderly individuals [19]. However, it is unclear that the molecular mechanism of the ageing process affects mitochondrial function, contributing to the development of osteoarthritis.

Mitochondria, as semiautonomous organelles, can translate 13 proteins encoded by the mitochondrial genome [20,21]. Most proteins in mitochondria are encoded by nuclear genes, which are translated in the cytoplasm, imported into mitochondria and are responsible for maintaining and regulating the normal functions of mitochondria [22]. The relationship between nuclear-encoded mitochondrial functional protein changes and osteoarthritis has not been deeply studied. In this study, we found that the expression of Lon protease 1 (LONP1) was downregulated in OA and that knockdown of LONP1 exacerbated the development and progression of osteoarthritis by inducing mitochondrial dysfunction in articular cartilage. LONP1 is a nuclear DNA-encoded mitochondrial enzyme that has been highly conserved throughout evolution and has functions in the degradation of damaged proteins, the correct folding of proteins imported into mitochondria and the regulation of mitochondrial gene expression, playing an important role in mitochondrial protein quality control (MQC) [23,24]. We also unravel the underlying molecular mechanism of LONP1 knockdown, which involves activation of the downstream MAPK pathway, an important signalling pathway in osteoarthritis [25,26]. Resveratrol (Res), as an antioxidant, inhibits the overexpression of mitochondrial ROS and the activation of the MAPK pathway after LONP1 knockdown, which can alleviate the progression of osteoarthritis. Understanding the biological mechanisms behind LONP1 downregulation can not only provide new insights into disease pathogenesis but also lead to the development of new treatments that slow or stop disease progression. Research has shown that LONP1 downregulation is associated with ageing and cell senescence [27–30]. This phenomenon have been confirmed in aged rat cartilage and senescent chondrocytes we speculate that ageing-induced LONP1 downregulation is an important factor contributing to osteoarthritis.

2. Materials and methods

2.1. Reagents

Foetal bovine serum (FBS), penicillin/streptomycin, Dulbecco's modified Eagle's medium (DMEM), and 0.25% trypsin were purchased from Gibco BRL. Collagenase II was purchased from Sigma–Aldrich, and recombinant rat interleukin-1β (IL-1β) was purchased from R&D Systems. Lentiviral LONP1 overexpression particles (Lenti-OE), overexpression control particles (ctrl-OE), lentiviral LONP1 knockdown particles (Lenti-KD), and knockdown control particles (ctrl-KD) were produced by and purchased from Cyagen (Suzhou, China).

2.2. Human samples

This study was in accordance with the Helsinki Declaration (2000) and approved by the Ethics Committee of the 2nd Affiliated Hospital, School of Medicine, Zhejiang University, Hangzhou, China (No. 20211127). OA-group cartilage samples were obtained from 11 patients (7 females, 4 males; mean age: 67 years; age range: 60–78 years) with hip osteoarthritis who underwent total hip arthroplasty (THA). Normal (Nor)-group samples were collected from 11 patients (8 females, 3 males; mean age: 69 years; age range: 63–80 years) with femoral neck fractures who received THA within 3 days. All patients signed relevant informed consent forms before the operative procedure. Three samples from each of the two groups were used for RNA-seq analysis, and the remaining samples were used for Western blot (WB) analysis.

2.3. Cell isolation, culture and treatment

This study was approved by the Institutional Animal Care and Use Committee of Zhejiang University (Hangzhou, China). Knee articular cartilage obtained from 4-week-old Sprague–Dawley (SD) rats was cut into small pieces and digested with 0.25% trypsin-EDTA solution for 30 min. After being filtered and centrifuged (1000 rpm for 5 min), the isolated cartilage was digested with 0.2% collagenase II for 4 h at 37 °C. The chondrocytes were then seeded into 25 cm^2 flasks containing DMEM/F12 (10% FBS, 1% penicillin/streptomycin). These chondrocytes were considered passage-0 (P0) chondrocytes. When the cells reached approximately 90% confluence, the chondrocytes were passaged at a ratio of 1:3, and P1-3 cells were used in our study.

The process of infection was as follows: chondrocytes were incubated with lentiviral particles (1×10^8 TU/mL) and polybrene (1 mg/ml) in growth medium, and the infection medium was replaced with growth medium after 12 h. After that, chondrocytes with LONP1 knockdown for 1 day (Lenti-KD 1 day) and 3 days (Lenti-KD 3 days) were used for further experiments. Chondrocytes transfected with knockdown control particles for 1 day were used as a blank control (NC) group. To explore the role of LONP1 in the inflammatory environment in vitro, we used LONP1-knockdown or LONP1-overexpressing chondrocytes under the stimulation of IL-1β for 24 h after 1 day of transfection.

2.4. RNA-seq analysis

Three human cartilage samples from the Nor group and OA group were processed and submitted for RNA sequencing, namely, Nor 1–3 and OA 1–3. The cartilage specimens were frozen and pulverized into powder in liquid nitrogen, and total RNA was extracted using TRIzol (Invitrogen, Carlsbad, CA, USA) according to the manufacturer's instructions. To analyse the changes in rat chondrocytes induced by LONP1 knockdown, three rat samples from the NC group and LONP1-KD group were processed and submitted for RNA sequencing, namely, NC 1–3 and LONP1 KD 1–3. The rat chondrocytes of the NC group and LONP1-KD group were collected 3 days after transfection with knockdown control particles and knockdown lentiviral LONP1 particles, and total RNA was extracted using TRIzol (Invitrogen, Carlsbad, CA, USA) according to the manufacturer's instructions. Subsequently, total RNA was qualified and quantified using a NanoDrop and Agilent 2100 bioanalyzer (Thermo Fisher Scientific, MA, USA). An mRNA library was constructed by LC-Bio Technology Company, and sequencing files were generated with an Illumina NovaSeq™ 6000 (LC-Bio Technology Co., Ltd., Hangzhou, China).

2.5. Differential profiling and bioinformatics analysis

Differential expression analysis of raw counts was performed using the DEGSeq R package [31]. We defined genes with a fold change >2 or a fold change <0.5 and a P value < 0.05 as differentially expressed genes (DEGs). The Search Tool for the Retrieval of Interacting Genes (STRING) was used to perform integrated protein–protein interaction (PPI) network analysis of 111 DEGs that encode functional proteins located in mitochondria (http://string-db.org/) [32,33]. Cytoscape software (version 3.5) was used to visualize the PPI network of Nor and OA-specific DEGs [34,35]. The hub genes were calculated and identified by using CytoHubba, and a betweenness algorithm was then used to identify hub genes.

GO analysis was performed to elucidate the biological implications of the differentially expressed genes between the NC group and the LONP1-KD group, including the associated biological process (BP), cellular component (CC), and molecular function (MF) [36]. The analysis was performed using the org.Rn.eg.db package and the clusterProfiler 4.0 package. A false discovery rate (FDR) < 0.05 and a |LogFC|>2 were used as the cut-off criteria, and the top 10 GO terms were sorted by FDR value. Pathway analysis was used to identify the significantly influenced pathways associated with the differentially expressed genes according to the Kyoto Encyclopedia of Genes and Genomes (KEGG) database [37]. The threshold of significance was defined by a P value < 0.05 and a q value < 0.05. Gene set enrichment analysis (GSEA) was used to further identify the significantly enriched pathways. GSEA was conducted between the NC group and the LONP1-KD group, and an |NES|>1, a NOM P value < 0.05, and an FDR q-val<0.25 were set as the cut-off criteria.

2.6. Western blot analysis

Harvested human cartilage tissues were ground with a tissue homogenizer, and treated chondrocytes were extracted with RIPA lysis buffer (BeyondTime) containing protease and phosphatase inhibitors for 60 min. The IL-1β-treated rat chondrocytes mentioned above were then lysed with RIPA lysis buffer containing protease and phosphatase inhibitors for 60 min according to the manufacturer's instructions. Mitochondrial proteins were extracted from chondrocytes using a mitochondrial extraction kit (Beyotime, C3601). After quantification with a BCA Protein Assay kit, the hydrolysates were separated via 10% sodium dodecyl sulfate-polyacrylamide gels and transferred onto nitrocellulose membranes. The membranes were blocked with 5% BSA for 1 h at room temperature and cut into sections according to the relative molecular weights of different proteins. After incubation with primary antibodies at 4 °C overnight, the membranes were incubated with secondary antibodies for 2 h before measurement with a chemiluminescence imager (AI800, USA) using FDbio-Femto ECL (Fudebio, Hangzhou, China). Quantity One software (Bio-Rad) was used to quantify the intensity of each band. The antibody information is listed in Supplementary Table S1.

2.7. Mitochondrial membrane potential

After the NC group was transfected with knockdown control particles for 1 day and the Lenti-KD group was transfected with LONP1-knockdown particles for 1 or 3 days (Lenti-KD 1 day and Lenti-KD 3 days), the mitochondrial membrane potential of the NC group and Lenti-KD group was detected using JC-1 dye (3520-43-2, Sigma). Briefly, chondrocytes were digested, resuspended and incubated with 1X JC-1 dye in the dark for 15 min at 37 °C in a CO_2 incubator. After centrifugation and three washes with warm PBS, the cells (5×10^5/ml) were resuspended and analysed by flow cytometry using a 488 nm laser. The cumulative percentage of dye was calculated by FlowJo software.

2.8. Mitochondrial DNA content assay

Total DNA was isolated from chondrocytes using a DNeasy Blood and Tissue Kit (Qiagen) according to the manufacturer's instructions. Quantitative PCR was performed using the efficiency-adjusted ΔΔCT method for mitochondrial DNA-encoded cytochrome *c* oxidase subunit I (COXI) (primers: forward 5′-AGCCGGGGTGTCTTCTATCT-3′, reverse 5′-TGGGTTATAGCAGGGGGTTT-3′) and subunit II (COXII) (primers: forward 5′-ACAAGCACAATAGACGCCCA-3′, reverse 5′-GGGAGGGAAGGGCGATTAGA-3′) and nuclear-encoded 18S ribosomal DNA (18S rDNA) (primers: forward 5′-CCTGAGAAACGGCTACCACA-3′, reverse 5′-ACCAGACTTGCCCTCCAATG-3′). The thermocycling profiles started with 1 cycle of 95 °C incubation for 60 s followed by 40 cycles of 95 °C for 15 s, 60 °C for 15 s, and 72 °C for 30 s. The ratio of COXI or COXII DNA copy number to 18S rDNA represents the relative mitochondrial copy number.

2.9. ROS measurement

A Reactive Oxygen Species Assay Kit (Beyotime, China) was used to evaluate the intracellular ROS levels of chondrocytes. Each group was incubated with 10 μmol/L 2′,7′-dichlorofluorescein diacetate (DCFH-DA) at 37 °C for 20 min and then washed twice with serum-free medium. The ROS levels were detected under a confocal microscope at 485 nm. Mitochondrial ROS were detected by MitoSOX Red staining based on a standard protocol (M36008, InvitrogenTM). Chondrocytes were plated in complete growth medium with 5 μmol L^{-1} MitoSOX for 20 min at 37 °C in the dark. After washing with warm PBS, the cells were imaged with an inverted fluorescence microscope.

2.10. ATP measurements

After chondrocytes were separately treated as described above, the cellular ATP content of the NC group, Lenti-KD 1day group and Lenti-KD 3day group was measured using an ATP Assay Kit (Beyotime Biotechnology, Shanghai, China) according to the manufacturer's instructions. The values were detected by using a luminometer.

2.11. Mitophagy detection

After chondrocytes were separately treated as described above, a Mitophagy Detection Kit® (Dojindo Molecular Technologies, Kumamoto, Japan) was used to detect mitophagy in the NC group, Lenti-KD 1day group and Lenti-KD 3day group following the manufacturer's instructions. Briefly, the chondrocytes were first washed with serum-free medium twice, an appropriate volume of 100 nmol/l Mtphagy Dye

working solution was added, and the cells were incubated at 37 °C for 30 min. After that, the chondrocytes were washed with serum-free medium twice and incubated at 37 °C for 30 min with 1 μmol/l Lyso Dye working solution. After washing with serum-free medium twice, the chondrocytes were scanned with a confocal fluorescence microscope.

2.12. Mitochondrial morphometry

Morphological changes in mitochondria in LONP1-knockdown chondrocytes were observed using live cell fluorescence microscopy (Leica DMI6000, Leica Germany). For live-cell staining, chondrocytes were labelled with CellLight® Mitochondria-RFP (Invitrogen) for 24 h according to the manufacturer's protocol. After that, these chondrocytes were infected with lentiviral LONP1-knockdown particles for 12 h, and the infection medium was replaced with growth medium. Live-cell images were obtained on a Leica laser confocal microscope via an oil-immersion objective in a temperature-controlled chamber (37 °C, 5% CO_2). Images were automatically captured every 1 h for 3 consecutive days.

2.13. Transmission electron microscope (TEM) analysis

Chondrocytes transduced with lentiviral LONP1-knockdown particles or knockdown control particles for 3 days were fixed in 2.5% glutaraldehyde for 3 h. After that, the cells were fixed with 1% osmium tetroxide for 1 h at room temperature in the dark. The samples were then dehydrated with increasing ethanol concentrations (30–100%), immersed in propylene oxide, and embedded in Epon-812. Ultrathin sections were acquired via a Leica UC7 ultramicrotome and sequentially stained with uranyl acetate and lead nitrate. The processed samples were imaged with a JEM-1230 transmission electron microscope.

2.14. Measurement of chondrocyte oxygen consumption rate (OCR)

An Oxygraph-2k (O2k; OROBOROS Instruments, Innsbruck, Austria) was used to measure the OCR in intact chondrocytes. Approximately 1 $\times$ 10^6 cells/ml were suspended in MiR05. Measurements were performed under basal conditions and then after injections of 1 mM oligomycin, 1.0 mM carbonyl cyanide 4-trifluoromethoxyphenylhydrazone (FCCP) and antimycin A/rotenone (0.5 mM of both). The data were normalized to the cell concentrations following instructions provided by the manufacturer.

2.15. Measurement of cellular OXPHOS complex activity

To measure in situ respiratory complex activity, we employed an Oxygraph-2k using the chondrocytes in the Lenti-NC group, Lenti-KD 1day group and Lenti-KD 3day group as described above. Briefly, cells were washed with serum-free medium and added to each chamber containing 2 ml of MiR05. After that, the cells were treated with plasma membrane permeabilizer (Digitonin) (20 μg/10^6 cells) to initiate the experiment. ETC complex inhibitors and substrates were added sequentially to the chambers as follows: PMG (pyruvate: 5 mM, malate: 5 mM, glutamate: 10 mM), ADP (1 mM), cytochrome *c* (10 μM), rotenone (0.5 μM), succinate (10 mM), antimycin A (2 μM), AS + TMPD (ascorbate: 2 mM + N,N,N′,N'-tetramethyl-*p*-phenylenediamine: 0.5 μM), and AZD (100 mM). The readings after adding cytochrome *c* were considered the baselines. Complex I activity was determined as the difference between the OCR at baseline and after Complex I inhibition by rotenone. The activity of complexes II + III was determined as the difference in OCR after the addition of complex II substrate (succinate) and the inhibition of complex III (antimycin A). Complex IV activity was determined by directly adding AS + TMPD. The OCR values were normalized to the cell concentrations.

2.16. Senescence assay

A β-Galactosidase Activity Assay (Beyotime Biotechnology, Shanghai, China) was performed to measure cellular senescence according to the corresponding instructions.

2.17. Animal model

2.17.1. Investigating the role of LONP1 in the progression of OA in a rat model

Forty male Sprague–Dawley rats (200–250 g, 6 weeks old, specific pathogen free [SPF]) received destabilization of the medial meniscus (DMM) surgery and were considered OA rats, while 10 male Sprague–Dawley rats received sham surgery as a blank control (sham group). The OA rats were randomly divided into four groups: the Ctrl-OE group, Lenti-OE group, Ctrl-KD group and Lenti-KD group (10 rats in each group). These four groups received an intra-articular injection of 40 μl of lentiviral LONP1-knockdown particles, knockdown control particles, lentiviral LONP1-overexpressing particles, and overexpression control particles (1 $\times$ 10^8 TU/mL) in sequence 1 week post-operation. All rats were euthanized at 10 weeks post-operation, and these knee specimens were used for further analysis.

2.17.2. Therapeutic effect of resveratrol on LONP1 knockdown-induced osteoarthritis

To further test the therapeutic effect of Res in vivo, 30 Sprague–Dawley rats (200–250 g, 6 weeks old) that underwent DMM surgery were randomly divided into 3 groups, namely, the Ctrl-KD group, Lenti-KD group, and Lenti-KD + Res group. Forty microlitres of lentiviral LONP1-knockdown particles (1 $\times$ 10^8 TU/mL) were injected intra-articularly into OA rats in the Lenti-KD group and Lenti-KD + Res group at 1 week post-surgery. Knockdown control particles at the same dose were injected intraarticularly into OA rats in the NC-KD group. After knockdown lentivirus infection at 1 week post-surgery, the rats in the Lenti-KD + Res group were subjected to intra-articular injection of 40 μL of Res (20 μmol/ml) every 3 weeks, and the rats in the NC-KD group and Lenti-KD group were injected with 40 μL of PBS as a control. All rats were euthanized at 10 weeks post-operation, and these knee specimens were used for further analysis.

2.17.3. Age-related spontaneous knee OA rat model

Thirty male Sprague–Dawley rats were used for the ageing study in compliance with an approved protocol by the Ethics Committee of The Second Affiliated Hospital, School of Medicine, Zhejiang University and according to the National Institutes of Health guidelines (National Research Council (US) Institute for Laboratory Animal Research. Guide for the Care and Use of Laboratory Animals. National Academies Press, 1996). All rats were housed 5 animals/cage at room temperature (24 $\pm$ 2 °C) and at a relative humidity of 55 $\pm$ 5% with controlled lighting (12-h dark/12-h light cycle). During the experiment, the rats were allowed ad libitum access to feed and water. The ageing study was long-term (up to 24 months of age), and 10 random rats were sacrificed at 3, 12 and 24 months.

2.18. Histopathologic analysis

2.18.1. Micro-CT analysis

Briefly, joint specimens were fixed in 4% paraformaldehyde (PFA) and stored in 70% ethanol. The knee joints of rats were imaged by high-resolution micro-CT (80490, MILabs BV, Netherlands) with an isometric resolution of 20 μm and analysed by three-dimensional model visualization software (IMALYTICS Preclinical, version 2.1). In addition, quantitative morphometry indices of subchondral bone were evaluated by microtomographic data, including the trabecular thickness (Tb.Th), bone volume fraction (BV/TV), and trabecular separation (Tb.Sp).

2.18.2. Safranin O-Fast Green staining

The knee joints were decalcified with 10% EDTA for 2 months after fixation with 4% paraformaldehyde for 24 h. The specimens were dehydrated using an ascending ethanol series and embedded in paraffin blocks. Next, continuous paraffin sections (thickness: 5 μm) were prepared, and some tissue sections were stained with safranin O-Fast Green. Moreover, the OA cartilage histopathology assessment system (OARSI score) with a grading method (0–24) was used to evaluate the sections [38].

2.18.3. Immunohistochemistry

The hydrated knee joint tissue sections were first permeabilized for 5 min with 0.1% v/v Triton X-100, subjected to trypsin enzymatic antigen retrieval (Cat# ab970; Abcam) and then inactivated with hydrogen peroxide for 20 min. After being blocked with 5% BSA for 1 h, the sections were incubated with primary antibodies against COL2, aggrecan, P53, P16, and MMP13 at 4 °C overnight and then incubated with HRP-conjugated secondary antibodies. After that, the sections were visualized with a DAB chromogenic reagent kit (AR1021, Boster, China) and haematoxylin. The results were visualized using optical microscopy, and ImageJ software was used to quantify the positively stained cells. The antibody information is listed in Supplementary Table S1.

2.18.4. Immunofluorescence

Hydrated knee joint tissue sections were permeabilized for 5 min with 0.1% v/v Triton X-100, blocked with 5% BSA for 1 h and incubated with a primary antibody against LONP1 at 4 °C overnight. After washing thrice in PBS, the sections were incubated with corresponding fluorescent secondary antibodies and DAPI for 2 h in the dark and then visualized under a fluorescence microscope. The antibody information is listed in Supplementary Table S1.

2.19. Statistical analysis

All data values are shown as the mean ± SD. Statistical analysis was performed using GraphPad Prism software version 6.0 (GraphPad Software). Two groups were compared by Student's *t*-test, and more than two

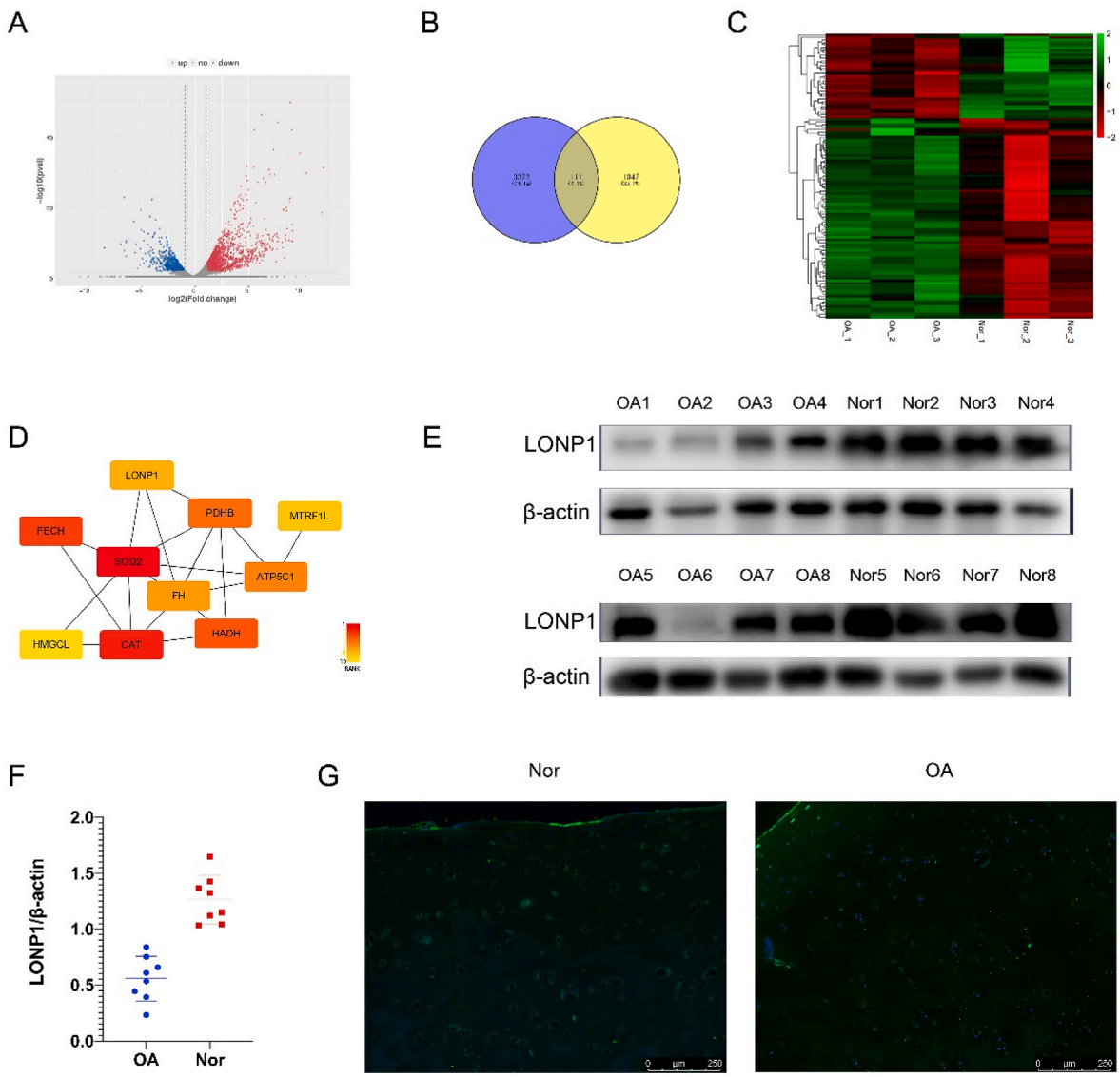

Fig. 1. A. Volcano plot of DEGs between the Nor group and the OA group. B. Venn diagram showing the intersection of DEGs and the MitoCarta 2.0 database. C. Hierarchical clustering illustrating the distinguished expression differences in Fig. 1B. D. Selected modules for the 10 highest hub gene connections after PPI interaction network analysis. E. Western blot analysis of LONP1 in human articular chondrocytes from hip osteoarthritis (OA) and fracture patients (Nor). F. The protein concentrations were detected by Western blot analysis. G. Immunofluorescence staining for LONP1 in human articular chondrocytes from hip osteoarthritis (OA) and fracture patients (Nor).

groups were compared by one-way ANOVA followed by Tukey's post-test. A value of $P < 0.05$ was considered to indicate significant differences.

3. Results

3.1. LONP1 expression is decreased in human osteoarthritic cartilage

In Fig. 1A, the volcano plot shows the DEGs between osteoarthritic and nonosteoarthritic articular cartilage as determined by RNA-seq. Mitochondria are semiautonomous organelles, and there are numerous proteins encoded from nuclear genes regulating mitochondrial functions. MitoCarta2.0 is an inventory of genes encoding mitochondrial-localized proteins [39]. The Venn diagram shows the intersection of the DEGs and the MitoCarta2.0 genes (Fig. 1B), which was used to screen whether expression changes of genes encoding predicted mitochondria -localized proteins in the pathogenesis of osteoarthritis. In Fig. 1C, the heatmap shows 111 differentially expressed genes (DEGs) in the intersection Venn diagram between the two clusters. To better understand the interplay among the identified DEGs, we obtained PPI networks using the STRING tool. The PPI networks included 273 intersections and 111 nodes (minimum interaction score≥0.4, in Supplementary Fig. 1). Fig. 1D shows the top 10 hub genes based on the CytoHubba betweenness algorithm in Cytoscape (version 3.5). Among these top 10 hub gene sets, we found LONP1 in a relatively core position, which is a highly conserved serine peptidase playing an important role in mitochondrial function maintenance [40]. To further test whether the expression of LONP1 is different between osteoarthritic and nonosteoarthritic joints, we performed Western blot analysis on human articular cartilage. As shown in Fig. 1E and F, LONP1 expression was reduced in hip cartilage from osteoarthritis patients undergoing THA surgery compared to that from trauma patients. These observations were also confirmed by immunofluorescence staining, which similarly showed strong fluorescence signals in nonosteoarthritic cartilage and decreased fluorescence signals in osteoarthritic cartilage (Fig. 1G). Together, these findings suggest that downregulation of LONP1 expression is positively associated with OA.

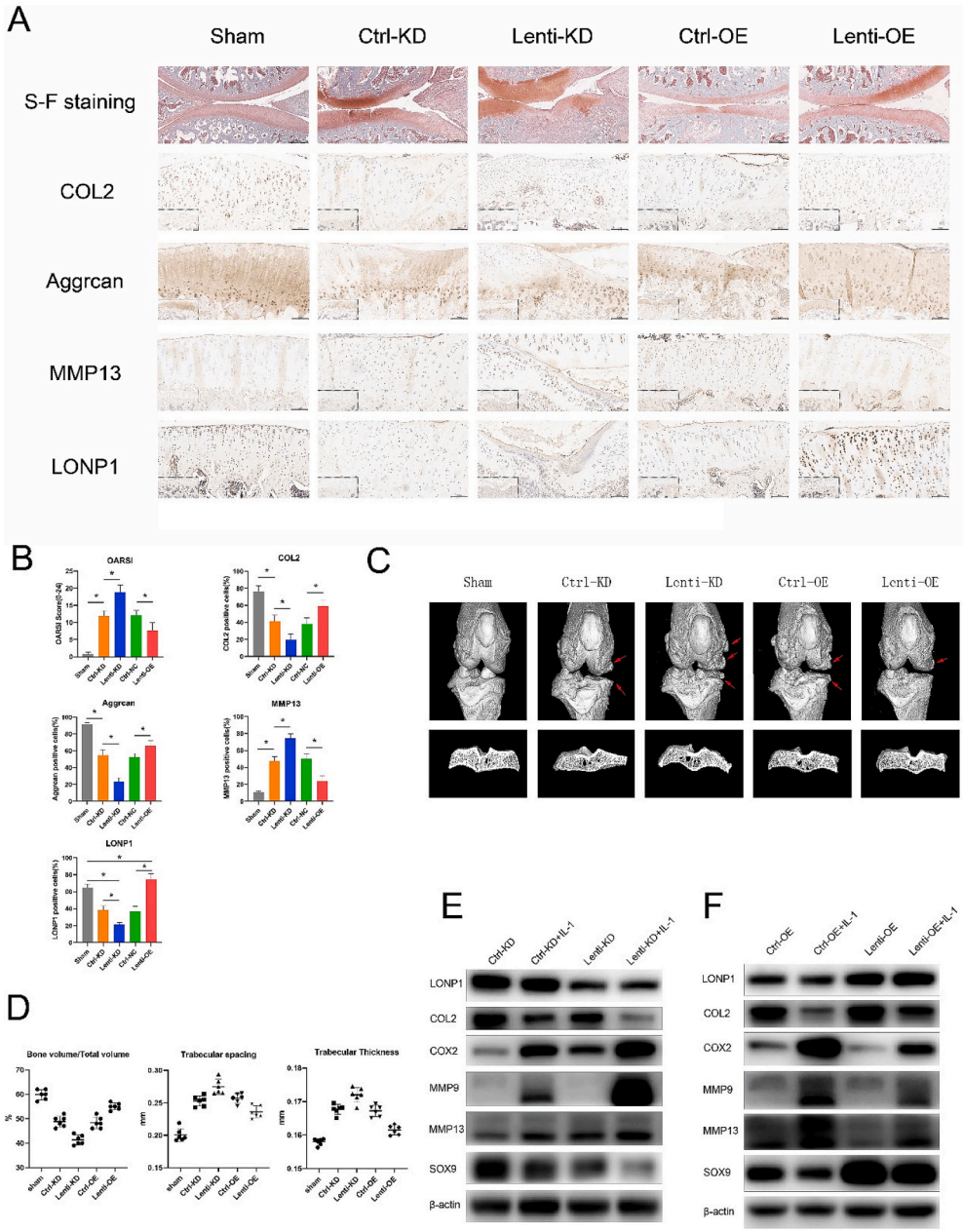

Fig. 2. A. Representative S–F staining and immunohistochemistry of knee joint sections from the five groups at 10 weeks post-surgery. B. OARSI scoring system (0–24) for S–F staining and quantification of positively stained cells by immunochemistry. (n = 6, *p < 0.05) C. Representative micro-CT images, including 3D images of osteophytes on the top and 2D images of subchondral bone on the bottom. D. Quantitative analysis of the volume fraction (BV/TV), trabecular spacing (Th.Sp.), and trabecular thickness (Tb.Th.) in MTP in the five groups 10 weeks post-surgery. E. Western blot analysis of the effects of LONP1 knockdown on IL-1β-induced COL2, COX-2, MMP9, MMP13, and SOX9 expression in rat chondrocytes. F. Western blot analysis of the effects of LONP1 overexpression on IL-1β-induced COL2, COX-2, MMP9, MMP13 and SOX9 expression in rat chondrocytes.

3.2. Effects of intra-articular LONP1 overexpression and knockdown on the rat OA model

LONP1, as a highly conserved protein, has >88% amino acid identity between human and rats, and the plot in green shows the highly conserved sequences between these species (Supplementary Fig. S2A). The spatial structure of the LONP1 protein in human and rat is shown in Figs. S2B and S2C. The rat OA model was induced by DMM surgery to investigate the potential impact of LONP1 on OA progression. We injected lentiviral LONP1-overexpressing particles (Lenti-OE) or lentiviral LONP1-knockdown particles (Len-KD) into the knee joints of rats to induce LONP1 overexpression or knockdown. This was performed in each group 1 week after DMM surgery. Immunofluorescence analysis of LONP1 was used to confirm the lentiviral transfection efficiency in the joints, which showed that the Lenti-OE group had even more LONP1-positive chondrocytes and that the Lenti-KD group had fewer (Fig. 2A and B). In addition, the number of LONP1-positive chondrocytes in the Ctrl-KD group and the Ctrl-OE group were much lower than the number in the sham group; this result is consistent with the result of human osteoarthritis showing that LONP1 expression is decreased in OA. As shown in Fig. 2A, S-F staining showed that the Lenti-OE group had considerably less cartilage destruction than the Ctrl-OE group, while the Lenti-KD group had more serious cartilage destruction. The OARSI score, as shown in Fig. 2B, was consistent with the above results. Furthermore, immunofluorescence analysis of MMP13, COL2 and Aggrecan was used to evaluate the development of OA. COL2 and Aggrecan, as important components of the cartilage matrix, are markers of anabolism. The number of COL2-and Aggrecan-positive cells was significantly higher in the Lenti-OE group than in the Ctrl-OE group and significantly lower in the Lenti-KD group than in the Ctrl-KD group. MMP13, a matrix-degrading enzyme, is a marker of cartilage catabolism. MMP13 expression was higher in the Lenti-KD group than in the Ctrl-KD group and lower in the Lenti-OE group than in the Ctrl-OE group.

Subsequently, microcomputed tomography (micro-CT) was used to evaluate osteophyte formation and subchondral bone changes in the five groups (Fig. 2C). Osteophytes protrude from the normal bone contour and have a reduced bone density, as indicated by red arrows in 3D images [41]. Among the five groups, the Lenti-KD group exhibited significantly more osteophytes than the Ctrl-KD group, and the Lenti-OE group exhibited significantly fewer osteophytes than the Ctrl-OE group. A cross-sectional view of subchondral bone can better reflect the activities of osteoblasts and osteoclasts in subchondral bone according to the formation of osteophytes and cavities, which indirectly reflect the severity of osteoarthritis. The subchondral bone volume fraction (BV/TV), trabecular spacing (Tb.Sp), and trabecular thickness (Tb.Th) of the medial tibial plateau (MTP) were investigated (Fig. 2D). The Lenti-KD group exhibited significantly lower BV/TV values but significantly higher Tb.Sp and Tb.Th values than the Ctrl-KD group, which showed that LONP1 knockdown can exacerbate subchondral bone remodelling. Compared with those of the Ctrl-OE group, the BV/TV value of the Lenti-OE group was significantly higher, but the Tb.Sp and Tb.Th values were significantly lower. Taken together, these results demonstrated that knockdown of LONP1 aggravated the progression of OA, while overexpression of LONP1 alleviated it.

3.3. Effect of LONP1 on IL-1β-induced inflammation in rat chondrocytes

To confirm these findings in vitro, we infected chondrocytes with Lenti-KD, Lenti-OE and their controls (Ctrl-KD and Ctrl-OE) before IL-1β (10 ng/ml) stimulation for 24 h. The efficiency of lentiviral transfection and the efficiency of knockdown/overexpression of LONP1 in chondrocytes as respectively determined by immunofluorescence and polymerase chain reaction (PCR) is shown in Fig. S3. As shown in Fig. 2E and Fig. S4A, WB analysis showed that the expression of matrix degradation-related proteins, including COX2, MMP9 and MMP13, was increased in the Lenti-KD group, while the expression of chondrogenesis-associated proteins, including COL2 and SOX9, was decreased in the Lenti-KD group. As shown in Fig. 2F and Fig. S4B, WB analysis showed that LONP1 overexpression alleviated the increases in COX2, MMP9 and MMP13 expression under IL-1 stimulation and reversed the decreases in COL2 and SOX9 expression, which was consistent with the results of the in vivo experiments.

3.4. LONP1 knockdown leads to mitochondrial dysfunction y

LONP1, as a key protein in MQC, can catalyse the degradation of misfolded matrix proteins and regulate mitochondrial gene expression to maintain normal mitochondrial function. To evaluate the function of mitochondria in chondrocytes after LONP1 knockdown, we examined mitochondrial function-related parameters such as mitochondrial membrane potential, mitochondrial ATP synthesis and mitochondrial mtDNA content.

Mitochondrial membrane potential (Δψ) is a sensitive marker of mitochondrial function, and a reduction in Δψ is associated with mitochondrial dysfunction. In Fig. 3A, the JC-1 flow cytometry analysis showed that the peak of LONP1-KD cells was shifted to the left compared to that of control cells, indicating a lower mitochondrial membrane potential. The ATP synthesis analysis showed that LONP1-KD chondrocytes had significantly lower ATP content than control cells (Fig. 3B). This result is consistent with mitochondrial depolarization, because Δψ stabilization is a prerequisite for oxidative phosphorylation, ATP production, and other mitochondrial functions. mtDNA encodes 13 mitochondrial respiratory chain proteins essential for OXPHOS, and the replication of mtDNA is essential for the cell to replenish damaged mitochondria and to maintain mitochondrial functionality [42]. The results in Fig. 3C show that LONP1 knockdown decreased the mitochondrial DNA content by approximately 1.25-fold for both COXI/18S rDNA and COXII/18S rDNA after 1 day and by approximately 2.5-fold for both COXI/18S rDNA and COXII/18S rDNA after 3 days.

3.5. LONP1 knockdown leads to mitochondrial MQC system dysfunction

The mitochondrial protease system, mitochondrial chaperone system, mitochondrial dynamics and mitophagy are all indispensable parts of the MQC system [43]. To further explore the effect of LONP1 knockdown on mitochondrial morphology and distribution, we cultured LONP1-knockdown chondrocytes with MitoTracker Red (Fig. 3D). We found that the elongated mitochondria became small, round punctate structures after 1 day of LONP1 knockdown. By 3 days of LONP1 knockdown, most mitochondria in chondrocytes had become small, round punctate structures or had disappeared. Mitochondrial dynamics is an important cellular process to maintain mitochondrial homeostasis that includes mitochondrial fusion and fusion, which are governed by mitochondrial fission and fusion proteins [44]. The functions of mitochondrial fission proteins such as DRP1 and Fis1 lead to mitochondrial fragmentation, which helps eliminate irreversibly damaged mitochondria. The functions of mitochondrial fusion proteins, such as MFN1, MFN2 and OPA1, lead to mitochondrial elongation, which is required to maintain and restore mitochondrial function by promoting the stochastic redistribution of soluble membrane components between normal and defective mitochondria [45,46]. With knockdown of LONP1, the levels of mitochondrial motility-related proteins were reduced, indicating that the regulation of mitochondrial motility could no longer reverse mitochondrial damage (Fig. 3E and F).

Mitophagy, as an important part of the MQC process, occurs when it is difficult for mitochondria to maintain their functions through regulation [47]. Some studies have revealed that PINK1 and Parkin work together to regulate mitophagy and mitochondrial biogenesis [48]. Mitophagy is stably initiated by PINK1 in dysfunctional mitochondria, and Parkin is then mobilized to mediate mitophagy [49]. In Fig. 3G, this mitophagy process is demonstrated by mitophagy staining under a confocal microscope. Mtphagy Dye binds to mitochondria in cells

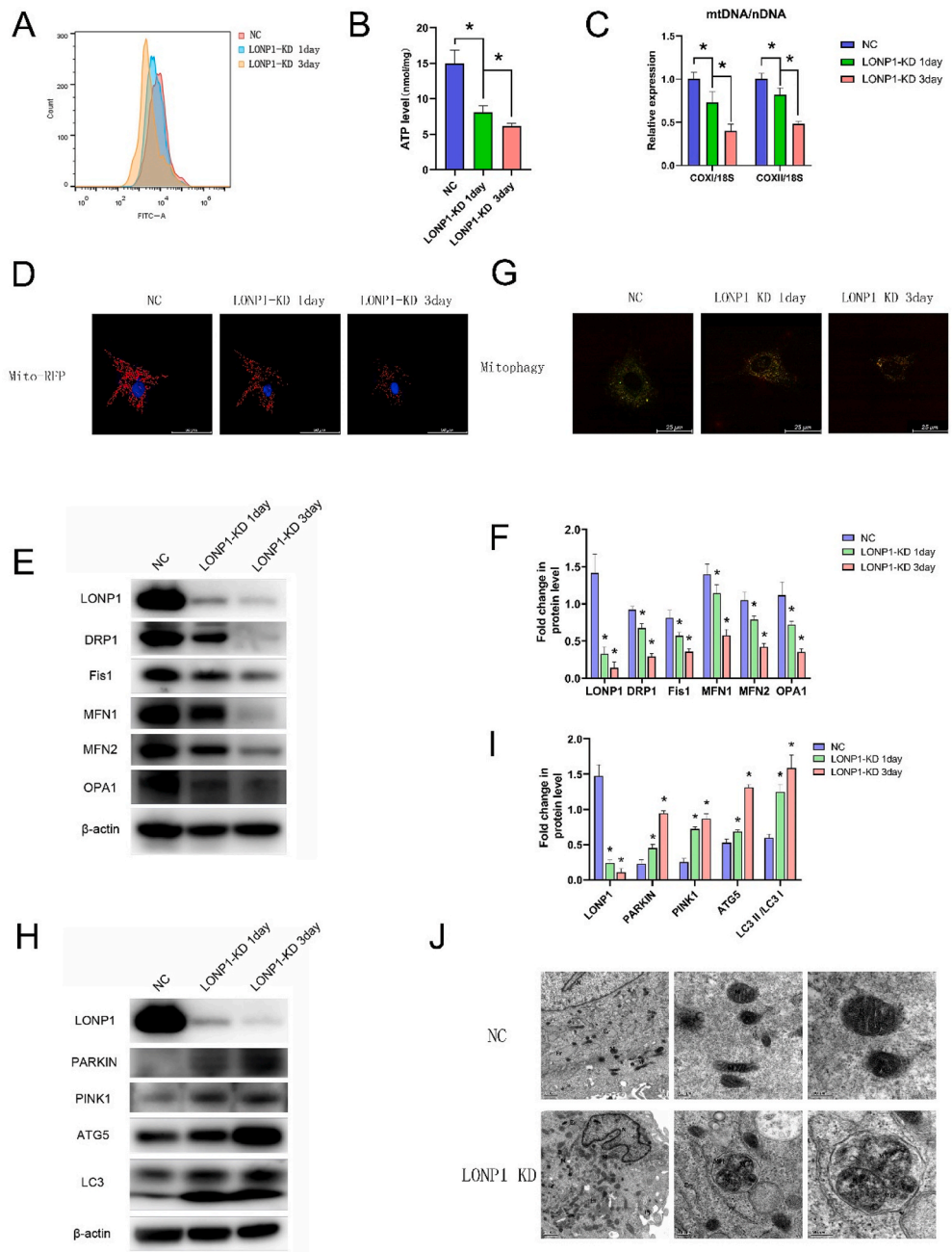

Fig. 3. A. Flow cytometry analysis of mitochondrial membrane potential as determined by JC-1 staining. B. ATP levels in chondrocytes from the NC group, LONP1-KD 1day group and LONP1-KD 3day group. The data are expressed as the mean ± SD. n = 3, *p < 0.05. C. Quantification of mtDNA in the NC group, LONP1-KD 1day group and LONP1-KD 3day group. The data are expressed as the mean ± SD. n = 3, *p < 0.05. D. Confocal images of the mitochondrial network from LONP1-knockdown chondrocytes (0–3 days) transfected with CellLight™ Mitochondria-GFP. E. Western blot analysis of mitochondrial fusion and fission in the NC group, LONP1-KD 1day group and LONP1-KD 3day group. F. Protein concentrations were detected by Western blot analysis. The data are expressed as the mean ± SD. n = 3, *p < 0.05. G. Confocal images of mitophagy staining of the NC group, LONP1-KD 1day group and LONP1-KD 3day group for Mtphagy Dye (red) and lysosomes (green). The colocalization of Mtphagy Dye Red with Lyso Dye (green) is shown in the merged images. H. Western blot analysis of mitochondrial autophagy-related proteins in the NC group, LONP1-KD 1day group and LONP1-KD 3day group. I. Quantification of the protein concentrations. The data are expressed as the mean ± SD. n = 3, *p < 0.05. J. TEM images of the NC and LONP1-knockdown groups. mt, mitochondria; ly, lysosome; e-pha, early phagosome; l-pha, late phagosome. (For interpretation of the references to colour in this figure legend, the reader is referred to the Web version of this article.)

through chemical bonds and maintains weak red fluorescence, and the fluorescence intensity of Mtphagy Dye increases by inducing fusion of mitochondria and autophagosomes when mitophagy occurs. Lysosomes were labelled green separately with Lyso Dye to confirm this process. The NC group had few red fluorescence signals with some green punctate lysosomal signals, indicating low levels of basal mitophagy. After 1 day of LONP1 knockdown, the red fluorescence signal of mitochondria in chondrocytes was enhanced, and an increased yellow signal was detected after fusion with the green fluorescence signal of lysosomes, suggesting that LONP1 deficiency triggers the mitophagy program. The yellow fluorescence signal was more pronounced in chondrocytes after 3 days of LONP1 knockdown, which indicates that knockdown of LONP1 in chondrocytes caused severe mitochondrial damage leading to mitophagy (Fig. 3G). As shown in Fig. 3H and I, WB analysis demonstrated that irreversible mitochondrial destruction led to increased expression of mitophagy-related proteins in LONP1-depleted chondrocytes. Specifically, in addition to the activation of the PINK–PARKIN mitophagy pathway, corresponding increases in the levels of the autophagy-related proteins ATG5 and LC3II/LC3I were observed with an increasing number of LONP1 knockdown days. To further study this phenomenon, we also analysed LONP1-knockdown chondrocytes by TEM (Fig. 3J). Under TEM, the normal chondrocytes possessed round or ovoid mitochondria with defined cristae. After 3 days of LONP1 knockdown, the chondrocytes showed abundant cleared regions within the cytosol, and mitochondria presented severe disruption of the cristae with electrodense aggregates. In addition, a large number of autophagosomes enclosing damaged mitochondria appeared in LONP1-depleted chondrocytes after 3 days. All these irreversible changes led to mitochondrial dysfunction in chondrocytes, resulting in the occurrence of osteoarthritis.

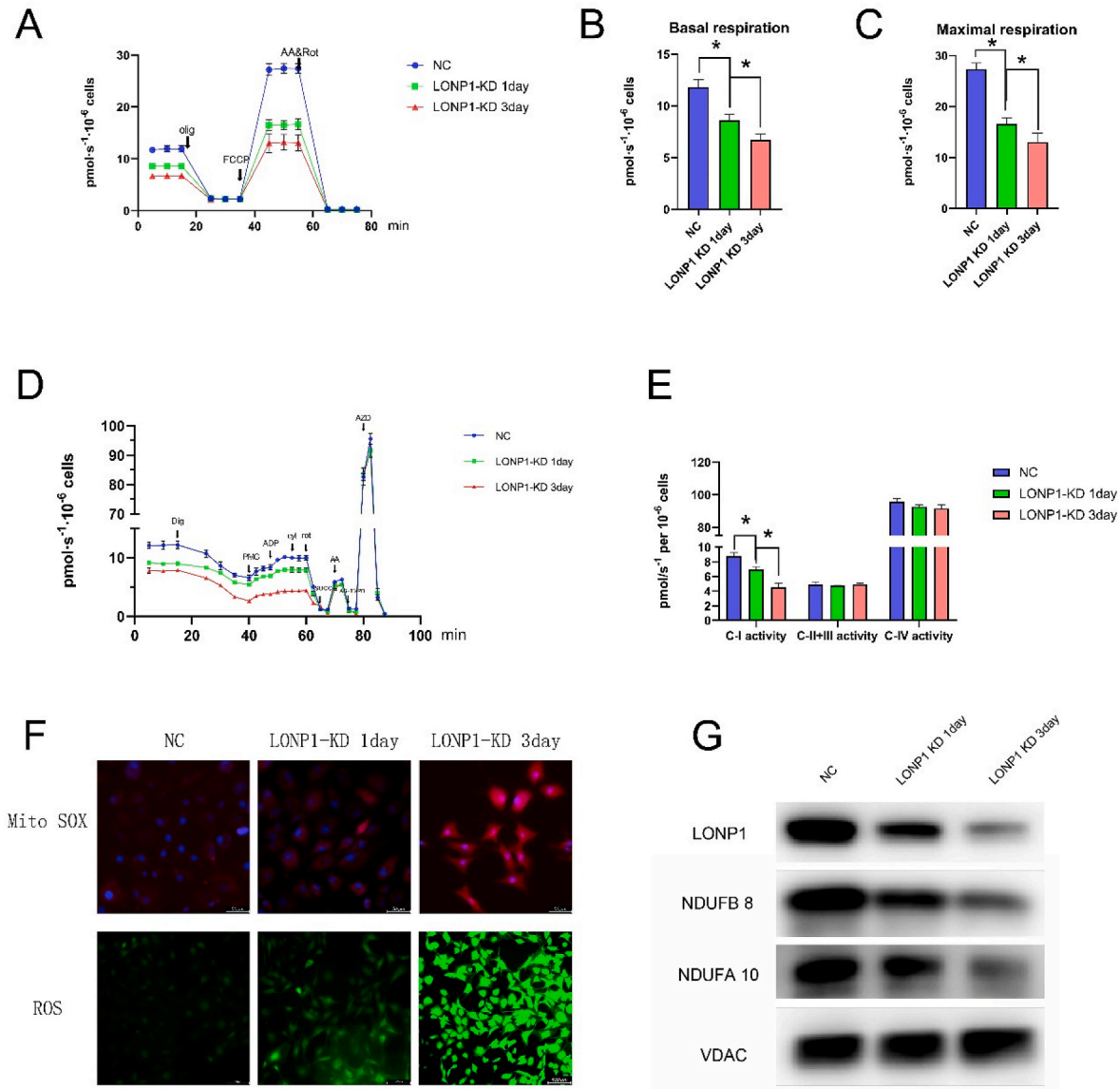

Fig. 4. A. OCR curves from the analysis of the effects of LONP1 knockdown on oxygen consumption of chondrocytes (blue: NC group, green: LONP1-KD 1day group, red: LONP1-KD 3 days) after the sequential addition of the indicated molecules. The data are expressed as the mean ± SD from three independent analyses. Olig: Oligomycin, FCCP: carbonyl cyanide 4-trifluoromethoxy-phenylhydrazone, AA&Rot: antimycin A & Rotenone. B. Basal respiration of chondrocytes from different groups measured over the first 15 min before the addition of any treatment. C. Maximal respiration of chondrocytes from different groups measured after FCCP treatment for 15 min until AA treatment was given. D. The mitochondrial respiration curve represents the function of the mitochondrial complex, which was measured by Oxygraph-2k after sequential addition of the indicated molecules. Dig: digitonin; PGM: pyruvate, glutamate and malate; ADP: adenosine diphosphate; Cyt: cytochrome *c*; Rot: rotenone; Succ: succinate; AA: antimycin A; AS, ascorbate; TEPD, tetramethyl-*p*-phenylenediamine dihydrochloride; AZD, sodium azide. The black arrows show when the substrates/reagents were injected. The data are expressed as the mean ± SD from three independent analyses. E. Complex-specific activities were quantified and were shown as a measurement of OCR. The data values are the mean ± SD. n = 3, *P < 0.05. F. Live cell staining of the NC group, LONP1-KD 1day group and LONP1-KD 3day group for ROS (green) and MitoSOX (red). G. Western blot analysis of the representative protein mitochondrial complex I. (For interpretation of the references to colour in this figure legend, the reader is referred to the Web version of this article.)

3.6. LONP1 knockdown dysregulates mitochondrial respiratory efficiency

To determine whether LONP1 KD in chondrocytes affects mitochondrial bioenergetics, we measured the mitochondrial OCR and function of the mitochondrial complex. The results in Fig. 4A-C shows that compared to NC chondrocytes, LONP1-KD chondrocytes showed significant decreases in basal OCR and maximal OCR over 1–3 days of LONP1 knockdown. These effects were accompanied by a significant decrease in spare respiratory capacity (SRC), defined as the difference between basal OCR and maximal OCR, which is an indicator of the ability of cells to cope with increased energy demand. Specific analysis of ETC complex activity in LONP1-KD chondrocytes showed that Complex I activity was significantly decreased compared to that in the controls, while Complex II + III and Complex IV activity was indistinguishable from that in the controls (Fig. 4D and E). Research has shown that reduced activity of Complex I is associated with increased reactive oxygen species (ROS) production [50,51]. In addition, recent research has shown that when Complex I is partially inhibited, electron flow through complex I will be blocked, and the generation of ROS will be intensified. However, when the function of complex I is severely impaired, the ROS produced by complex I will also be inhibited [52]. The analysis specifically measuring MitoSOX fluorescence staining showed that LONP1-KD chondrocytes had an increased level of superoxide generation, in a trend similar to that of total ROS in chondrocytes

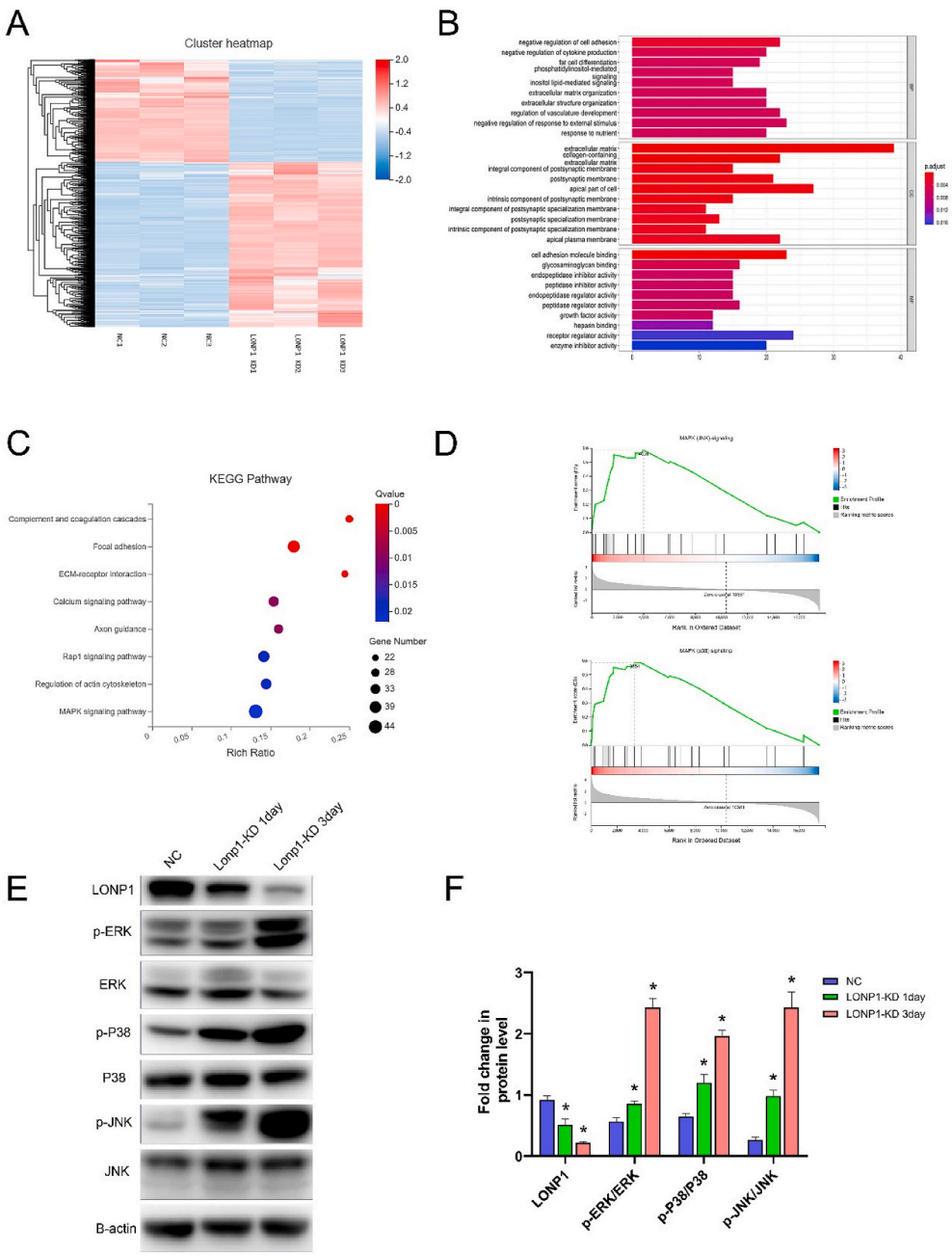

Fig. 5. A. Hierarchical clustering illustrating the distinguished expression differences of mRNA between the NC group and the LONP1-KD group. Red indicates genes with higher expression, and blue indicates genes with lower expression. B. GO functional classification of chondrocytes in the LONP1-KD group vs. the NC group. C. Top 10 most enriched KEGG pathways of the chondrocytes in the LONP1-KD group vs. the NC group. P value < 0.05 and q value < 0.05. D. GSEA of MAPK pathway-related genes. |NES|>1, NOM P value < 0.05, FDR q-val<0.25. E. Western blot analysis of MAPK pathway activation induced by LONP1 knockdown. F. Quantification of the protein concentrations. The data are expressed as the mean ± SD. n = 3, *p < 0.05. (For interpretation of the references to colour in this figure legend, the reader is referred to the Web version of this article.)

(Fig. 4F). Thus, we hypothesize that the partial reduction in mitochondrial respiratory complex I activity induced by LONP1 knockdown triggers mitochondrial ROS production in chondrocytes. NDUFB8 and NDUFA10 are involved in mitochondrial respiratory chain complex I assembly. WB analysis showed that the expression levels of NDUFB8 and NDUFA10 decreased with the knockdown of LONP1 compared with the levels of the internal reference VDAC (Fig. 4G and Fig. S5).

3.7. LONP1 knockdown induces MAPK pathway activation in chondrocytes

To analyse molecular-level changes in chondrocytes caused by LONP1 knockdown, we performed RNA sequencing on the samples of the NC group and the LONP1-KD group. The data were processed, and the 1947 differentially expressed genes under the standards of a $P < 0.05$ and a $|LogFC|>2$ are illustrated as a heatmap (Fig. 5A). Using the upregulated and downregulated gene sets identified in the comparative analysis of the NC group and LONP1-KD group, we performed an analysis with the Gene Ontology (GO) database, which is a repository of previously established gene lists annotated with terms related to different biological, cellular, or molecular characteristics [36]. As shown in Fig. 5B, the GO analysis showed that LONP1 knockdown significantly and severely affected the regulation of cell adhesion and the extracellular matrix in chondrocytes. In addition, KEGG pathway analysis also showed inhibition of focal adhesion and ECM–receptor interactions, and promotion of the MAPK signalling pathway in LONP1-knockdown chondrocytes (Fig. 5C). The MAPK signalling pathway is closely associated with inflammation, chondrocyte apoptosis and matrix degradation and has been reported to play an important role in osteoarthritis [25,26]. Because the MAPK pathway included both downregulated and upregulated genes in the analysis, we performed GSEA of the KEGG module to further test for enrichment in the MAPK signalling pathway.

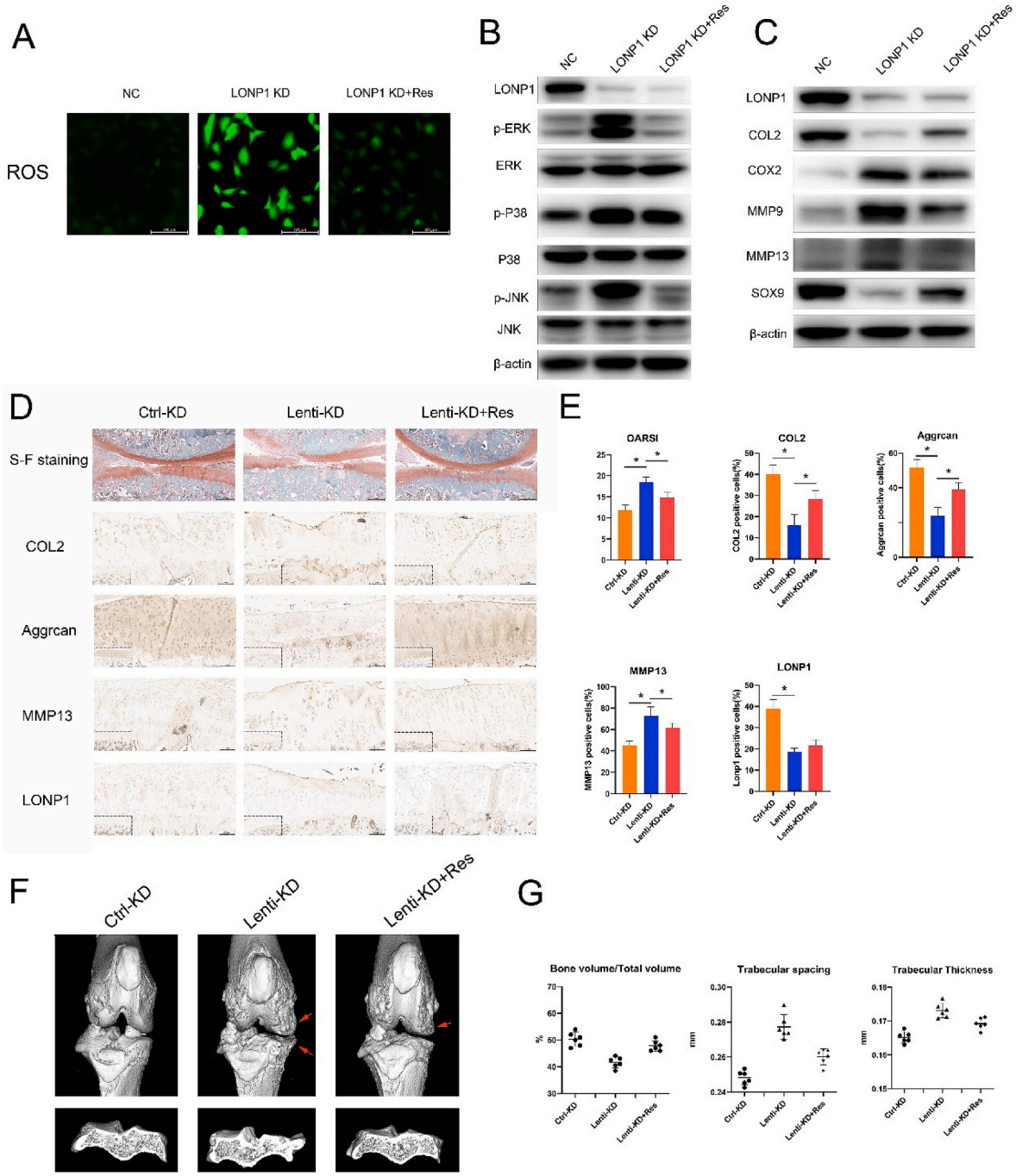

Fig. 6. A. The fluorescence diagram shows that Res reversed the effects of LONP1 knockdown on total ROS in chondrocytes. B. Western blot analysis showed that Res reversed the MAPK pathway activation caused by LONP1 knockdown. C. Western blot analysis showed that Res reversed the catabolism and maintained the anabolism caused by LONP1 knockdown. D. Representative S–F staining and immunohistochemistry of knee joint sections of the Crtl-KD group, Lenti-KD group and Lenti-KD + Res group. E. OARSI scoring system (0–24) for S–F staining and quantification of positively stained cells by immunochemistry ($n = 6$, $^*p < 0.05$) F. Representative micro-CT images, including 3D images of osteophytes on the top and 2D images of subchondral bone on the bottom. G. Quantitative analysis of the volume fraction (BV/TV), trabecular spacing (Tb.Sp.), and trabecular thickness (Tb.Th.) in MTP in the three groups.

The results in Fig. 6D show that the JNK pathway and P38 pathway were upregulated in the GSEA analysis of KEGG module, which further shows that knockdown of LONP1 can cause activation of the MAPK signalling pathway. The WB analysis results were consistent with the sequencing results, indicating that the MAPK pathway was activated in LONP1-knockdown chondrocytes (Fig. 6E and F). Taken together, these data reveal that knockdown of LONP1 can cause activation of the MAPK signalling pathway in articular cartilage.

3.8. Resveratrol eliminate ROS and inhibit the MAPK signalling pathway contributing to chondroprotection under LONP1 knockdown

Resveratrol is a natural polyphenol with antioxidant, anti-inflammatory, cardioprotective and anticancer properties as well as an inhibitor of the MAPK pathway [53–55]. As shown in Figs. 6A and 10 μM resveratrol significantly reversed the elevation in ROS levels induced by LONP1 knockdown in vitro. Next, we performed WB analysis to determine the effect of pharmacologic inhibition of MAPK with resveratrol, which

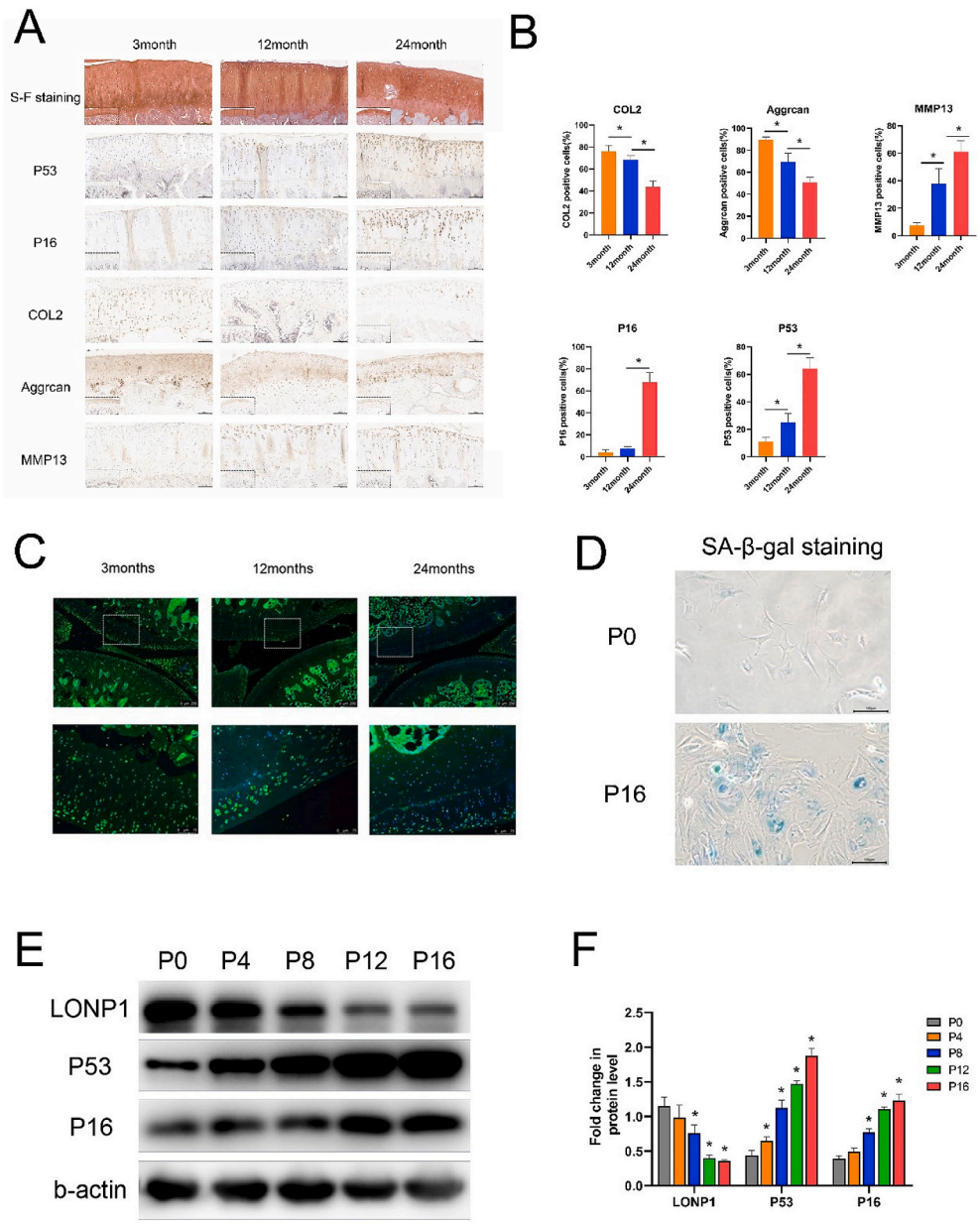

Fig. 7. A. Representative S–F staining and immunohistochemical staining of knee joint sections from young (3 months), middle-aged (12 months) and old (24 months) rats. B. OARSI scoring system (0–24) for S–F staining and quantification of positively stained cells by immunochemistry (n = 6, *p < 0.05) C. Representative images of immunofluorescence staining of LONP1 in knee joint sections of young (3 months), middle-aged (12 months) and old (24 months) rats. D. Representative images of SA-β-gal staining in chondrocytes at the 0th (P0), 4th (P4), 8th (P8), 12th (P12) and 16th (P16) passages. E. Western blot analysis of LONP1, P53, P16 and β-actin in chondrocytes at P0, P4, P8, P12 and P16. F. The protein concentrations were detected by Western blot analysis. The results are expressed as the mean ± standard deviation (n = 3, *p < 0.05 versus the P0 group).

showed that resveratrol can reverse the activation of the MAPK signalling pathway induced by LONP1 knockdown (Fig. 6B). In addition, resveratrol alleviated the increases in the expression of inflammation-related proteins such as MMP9, MMP13 and COX2 caused by LONP1 knockdown and mitigated the decreases in the expression of chondrogenesis-related proteins such as COL2 and SOX9 in LONP1-KD chondrocytes (Fig. 6C). To evaluate whether Res can alleviate osteoarthritis aggravated by LONP1 knockdown in vivo, we evaluated knee cartilage degradation in rats in the Ctrl-KD group, Lenti-KD group and Lenti-KD + Res group. As shown in Fig. 7D and E, S-F staining revealed that the knee sections of the Lenti-KD + Res group showed healthier cartilage and lower OARSI grades than those of the Lenti-KD group, while the knee sections of the Lenti-KD group showed disrupted and discontinuous cartilage with the highest OARSI grade compared to those of the Ctrl-KD group.

Immunohistochemical staining analysis showed that the number of cells stained positively for COL2 and Aggrecan was higher and that the number of cells stained positively for MMP13 was lower in the Res-treated group than in the Lenti-KD group (Fig. 6D and E), suggesting that resveratrol could relieve the aggravation of osteoarthritis caused by LONP1 knockdown. However, there was no difference in the number of LONP1-positive cells between the Res-treated group and the Lenti-KD group, which is consistent with the results of WB analysis. Compared with the Lenti-KD group, the Res-treated group exhibited reduced aggravation of osteophyte formation, but it is still more serious than Ctrl-KD group (Fig. 6F). The Lenti-KD group exhibited obvious subchondral bone changes, with the highest Th.Sp., Tb.Th. and the lowest BV/TV among these three groups. Notably, the Th.Sp. and Tb.Th. scores in the Res-treated group were significantly lower than those in the Lenti-KD group, and the BV/TV scores were similar to those in the Ctrl-KD group, suggesting a chondroprotective effect of Res in the LONP1-knockdown rat OA model (Fig. 6G).

3.9. LONP1 expression is downregulated in ageing cartilage and replicative senescence chondrocytes

Ageing is an important risk factor for the development of osteoarthritis, and understanding how the ageing process contributes to the development of osteoarthritis is an important area of research. Previous

studies have reported that LONP1 expression and activity decline with age, and genetic or ageing-associated imbalances in LONP1 activity are implicated in numerous human diseases associated with pathologic mitochondrial dysfunction [23,29,56,57]. However, the expression of LONP1 in ageing cartilage has not been reported. We next explored the changes in LONP1 expression during ageing, speculating that ageing may be a factor in LONP1 downregulation leading to osteoarthritis. A rat ageing model of young-adult (3 months), middle-aged (12 months), and old (24 months) rats was established to reveal the LONP1 protein expression in cartilage during ageing.

As shown in Fig. 7A, S-F staining indicated that cartilage thinning was accompanied by loss of cartilage matrix as well as cellular hypertrophy in the ageing rat model, and these results have also been shown in some similar studies [58,59]. In addition, chondrocyte hypertrophy is accompanied by cellular senescence, which is a set of cellular phenotypes that often coexist in a stressed environment [60]. Research has revealed that articular chondrocytes lose their differentiated phenotype under disease conditions and differentiate into cells in an endochondral ossification (EO)-like proliferative state with abnormal hypertrophy [61]. Compared with the cartilage layers of the rats at 3 months and 12 months, the cartilage layers of 24-month-old rats showed cavitation, which indicates the appearance of local calcification (Fig. 7A). This may be one of the manifestations of ageing in cartilage because hypertrophy and senescence are believed to precede ossification and mineralization, which occur along the endochondral ossification pathway [62,63]. P16 and p53 are markers of cellular senescence. Histochemical staining showed that the positive cell rates of p16 and p53 in 24-month-old rat chondrocytes were significantly higher than those of 6-month-old and 12-month-old rat chondrocytes; the positive rate of p16 was 68% in 24-month-old rat chondrocytes, and the positive rate for P53 was 62% (Fig. 7A and B). Histochemical staining showed that the positive staining of MMP13 in rat chondrocytes increased with ageing and that the positive rate of COL2 and Aggrecan staining decreased with ageing. Ageing cartilage has been shown to exhibit increased levels of matrix-degrading enzymes, such as MMP13, with ageing as well as age-related decreases in mature collagen expression [64–66]. Moreover, immunofluorescence analysis of LONP1 expression in young-adult, middle-aged, and old rat groups revealed that the expression of LONP1 was progressively downregulated during ageing (Fig. 7C). The above results indicates that the knee cartilage of rats presents manifestations of osteoarthritis with ageing and that LONP1 expression decreases gradually during the ageing process.

Chondrocytes divide in vitro and show the characteristics of telomere shortening in replicative senescence after multiple passages [67]. There is also evidence of telomere shortening in chondrocytes isolated from elderly individuals [68]. Senescence-associated β-galactosidase (SA-β-gal) is a widely used biomarker of senescent cells [69]. The expression of SA-β-gal in chondrocytes was determined by SA-β-gal staining as described (Fig. 7D), and SA-β-gal staining showed that compared to P0 chondrocytes, a large number of P16 chondrocytes showed senescence-related phenotypes. Chondrocytes are mostly in the stationary phase in mature cartilage in vivo, and expansion in vitro renders chondrocytes more prone to dedifferentiation and a senescent phenotype [68,70,71]. However, when osteoarthritis occurs, some chondrocytes will enter the proliferative phase from the stationary phase to repair the damaged cartilage in a self-repair mechanism due to the destruction of the extracellular matrix, and these cells are more susceptible to senescence. Through Western blot experiments of replicative senescent chondrocytes in vitro, we found that the expression of LONP1 protein decreased with replicative senescence, and the expression decrease in the P8–P12 generation was more obvious than that in the P0 generation (Fig. 7E and F).

4. Discussion

OA is the most common form of arthritis and a leading cause of disability in older adults [72]. Mitochondria are complex and dynamic organelles that not only produce energy but also participate in a variety of cellular physiological processes. An increasing number of experiments have shown that mitochondrial dysfunction is closely related to the occurrence and development of osteoarthritis. Wang et al. reported that mitochondrial biogenesis is impaired in osteoarthritic chondrocytes and that activation of the AMPK pathway can reverse impairments in mitochondrial biogenesis capacity [73]. Mitochondrial transplantation from normal cartilage can also ameliorate the development and progression of osteoarthritis [74]. In addition, mitochondrial dysfunction increases inflammatory responsiveness to cytokines in normal human chondrocytes, which may occur through ROS production and NF-κB activation [75]. Furthermore, some studies have shown that the core event of mitochondria-induced osteoarthritis is oxidative stress, which modulates matrix destruction through upregulation of MMP protein levels [76]. Mitoprotection, as a promising therapeutic strategy, can effectively relieve the development of OA [77].

Mitochondria, as semi-autonomous organelles, have their own mtDNA-encoded proteins, but most of the mitochondrial functional proteins are encoded in the nucleus. Through RNA-seq screening of normal and osteoarthritis human cartilage tissue and in vitro validation, we found that OA cartilage is characterized by a decrease in the expression of LONP1. LONP1 is a highly conserved serine peptidase that plays an important role in the protein quality control system in mammalian mitochondria [23,24]. We found lower expression of LONP1 in the damaged zone from OA cartilage than in the intact zone from the same individual in the rat DMM model. After that, we used lentiviruses to establish LONP1 overexpression/knockdown models in vivo and in vitro. The results suggest that LONP1 knockdown can exacerbate osteoarthritis progression in DMM models and upregulate the expression of inflammation-related genes, including COX2 and MMP13, in IL-1β-induced inflammation models. Moreover, overexpression of LONP1 has a protective effect against OA progression.

Multiple mechanisms are utilized by mitochondria to maintain their homeostasis, which is elaborately organized at the molecular level with chaperones and proteases [78,79], at the transcriptional level through the mitochondrial unfolded protein response (UPRmt) and the integrated stress response (ISR) [80,81], and at the organellar level by mitochondrial dynamics and mitophagy [82–84]. LONP1, as a kind of nuclear-encoded protease, plays an important role in the maintenance of mitochondrial homeostasis. To better understand the mitochondrial changes corresponding to LONP1 knockdown in OA, we used lentivirus-transfected chondrocytes to analyse mitochondrial function after LONP1 knockdown. Our study revealed a decrease in mtDNA, loss of mitochondrial membrane potential, mitochondrial fragmentation, and mitochondrial dynamics disruption. Consistent with the functional decrease in mitochondrial membrane potential, the amount of ATP production also decreased with LONP1 knockdown. In addition, knockdown of LONP1 leads to irreversible mitochondrial damage in chondrocytes and ultimately leads to massive mitophagy via the PINK1-PARKIN pathway. As a major mitochondrial protease, LONP1 also plays an indispensable role in metabolic programming by remodelling OXPHOS complexes and modulating OXPHOS activity [85,86]. Our work revealed that both basal respiration and maximal respiration were reduced in the LONP1-knockdown group compared to the blank group. There were significant increases in the levels of cellular ROS and mitochondrial peroxides, and significant reductions in the levels of Complex I subunits (Ndufa10 and Ndufb8). The reasons for these results may be the mitochondrial ETC complex I is an important site of ROS production and reduced activity of Complex I is associated with increased ROS production [87,88]. Furthermore, in our work, the results of RNA-seq for the LONP1-KD group and the NC group revealed that loss of LONP1 was positively associated with activation of the MAPK pathway. We assume that this was due to LONP1 knockdown resulting in a persistent excess of ROS activating the MAPK pathway [89,90]. Resveratrol, as an antioxidant, can alleviate the MAPK pathway activation caused by LONP1 knockdown-induced excessive ROS accumulation to alleviate the process of osteoarthritis in vitro and in vivo.

There is bidirectional communication between the nucleus and mitochondria in cells. This bidirectional communication includes anterograde regulation, which regulates mitochondrial biogenesis and activity through the nucleus, and retrograde regulation, which controls the nuclear epigenome and regulates nuclear genes through mitochondrial metabolites and signalling molecules produced by mitochondria [91]. The UPRmt, as a retrograde regulation pathway, promotes the synthesis of nuclear-encoded mitochondrial chaperones when the mitochondrial protein quality control system is insufficient to offset the accumulation of defective peptides under stress [92,93]. It is well accepted that ageing is an important contributing factor to the development of OA, and the abnormal gene expression regulated by epigenetic mechanisms in ageing cartilage affects age-related OA pathogenesis [94,95]. In our study, we found that LONP1 expression was decreased in both ageing cartilage and replicative senescent chondrocytes. Emerging evidence indicates that the ageing process alters nuclear gene expression through anterograde regulation, which results in LONP1 downregulation. This result affects mitochondrial function, leading to osteoarthritis occurrence. However, the potential LONP1 downregulation associated with epigenetic regulation should be further investigated. The mechanism of epigenetic regulation mediated by the ageing process resulting in genome expression changes should also be fully identified.

5. Conclusions

In summary, we have illustrated that the loss of LONP1 is associated with mitochondrial dysfunction in OA, which is positively associated with the ROS-activated MAPK pathway. In addition, our results reveal that ageing may be a predisposing factor for LONP1 downregulation, leading to the occurrence and development of osteoarthritis.

Author contributions

Yuzhe He, Qianhai Ding and Wenliang Chen designed this study, Study conduct: Yuzhe He, Changjian Lin and Lujie Ge. Analysis and interpretation of data: Kai Xu, Zhipeng Wu and Langhai Xu. Drafting the article: Yuzhe He, Qianhai Ding and Jisheng Ran. Revising manuscript content and approving final version of manuscript: Weiping Chen and Lidong Wu.

Declaration of interests statement

There are no conflicts of interest to declare.

Data availability

Data will be made available on request.

Acknowledgments

This research was supported by National Natural Science Foundation of China [grant number 81871793] and supported by Zhejiang Province Medical and Health project [grant number LD19H060001, LY19H060004].

Appendix A. Supplementary data

Supplementary data to this article can be found online at https://doi.org/10.1016/j.freeradbiomed.2022.08.038.

References

[1] J. Martel-Pelletier, A.J. Barr, F.M. Cicuttini, P.G. Conaghan, C. Cooper, M. B. Goldring, J.P. Pelletier, et al., Osteoarthritis, Nat. Rev. Dis. Prim. 2 (2016), 16072.
[2] H.A. Wieland, M. Michaelis, B.J. Kirschbaum, K.A. Rudolphi, Osteoarthritis - an untreatable disease? Nat. Rev. Drug Discov. 4 (2005) 331–344.
[3] J.W. Michael, K.U. Schlüter-Brust, P. Eysel, The epidemiology, etiology, diagnosis, and treatment of osteoarthritis of the knee, Dtsch Arztebl Int 107 (2010) 152–162.
[4] M. Chojnacki, A. Kwapisz, M. Synder, J. Szemraj, Osteoarthritis: etiology, risk factors, molecular mechanisms, Postepy Hig. Med. Dosw. 68 (2014) 640–652.
[5] S. Glyn-Jones, A.J. Palmer, R. Agricola, A.J. Price, T.L. Vincent, H. Weinans, A. J. Carr. Osteoarthritis. *Lancet* 386 (2015) 376–387.
[6] P.K. Sacitharan, Ageing and osteoarthritis, Subcell. Biochem. 91 (2019) 123–159.
[7] L. Habiballa, H. Salmonowicz, J.F. Passos, Mitochondria and cellular senescence: implications for musculoskeletal ageing, Free Radic. Biol. Med. 132 (2019) 3–10.
[8] R.F. Loeser, S.R. Goldring, C.R. Scanzello, M.B. Goldring, Osteoarthritis: a disease of the joint as an organ, Arthritis Rheum. 64 (2012) 1697–1707.
[9] S.Y. Jeong, D.W. Seol, The role of mitochondria in apoptosis, BMB Rep 41 (2008) 11–22.
[10] R. Bravo-Sagua, V. Parra, C. López-Crisosto, P. Díaz, A.F. Quest, S. Lavandero, Calcium transport and signaling in mitochondria, Compr. Physiol. 7 (2017) 623–634.
[11] R. Rizzuto, D. De Stefani, A. Raffaello, C. Mammucari, Mitochondria as sensors and regulators of calcium signalling, Nat. Rev. Mol. Cell Biol. 13 (2012) 566–578.
[12] F.J. Blanco, M.J. López-Armada, E. Maneiro, Mitochondrial dysfunction in osteoarthritis, Mitochondrion 4 (2004) 715–728.
[13] F.J. Blanco, R.K. June, 2nd. Cartilage metabolism, mitochondria, and osteoarthritis, J. Am. Acad. Orthop. Surg. 28 (2020) e242–e244.
[14] L.Y. Chen, Y. Wang, R. Terkeltaub, R. Liu-Bryan, Activation of AMPK-SIRT3 signaling is chondroprotective by preserving mitochondrial DNA integrity and function, Osteoarthritis Cartilage 26 (2018) 1539–1550.
[15] M.D. Carlo Jr., R.F. Loeser, Increased oxidative stress with aging reduces chondrocyte survival: correlation with intracellular glutathione levels, Arthritis Rheum. 48 (2003) 3419–3430.
[16] L. Wu, H. Liu, L. Li, H. Liu, Q. Cheng, H. Li, H. Huang, Mitochondrial pathology in osteoarthritic chondrocytes, Curr. Drug Targets 15 (2014) 710–719.
[17] F.J. Blanco, I. Rego, C. Ruiz-Romero, The role of mitochondria in osteoarthritis, Nat. Rev. Rheumatol. 7 (2011) 161–169.
[18] H. Martini, J.F. Passos, Cellular senescence: all roads lead to mitochondria, FEBS J. (2022), https://doi.org/10.1111/febs.16361.
[19] J. Birch, J.F. Passos, Targeting the SASP to combat ageing: mitochondria as possible intracellular allies? Bioessays 39 (2017).
[20] B.M. Hällberg, N.G. Larsson, Making proteins in the powerhouse, Cell Metabol. 20 (2014) 226–240.
[21] S. Anderson, A.T. Bankier, B.G. Barrell, M.H. de Bruijn, A.R. Coulson, J. Drouin, I. G. Young, et al., Sequence and organization of the human mitochondrial genome, Nature 290 (1981) 457–465.
[22] O. Schmidt, N. Pfanner, C. Meisinger, Mitochondrial protein import: from proteomics to functional mechanisms, Nat. Rev. Mol. Cell Biol. 11 (2010) 655–667.
[23] D.A. Bota, K.J. Davies, Mitochondrial Lon protease in human disease and aging: including an etiologic classification of Lon-related diseases and disorders, Free Radic. Biol. Med. 100 (2016) 188–198.
[24] L. Gibellini, A. De Gaetano, M. Mandrioli, E. Van Tongeren, C.A. Bortolotti, A. Cossarizza, M. Pinti, The biology of Lonp1: more than a mitochondrial protease, Int. Rev. Cell. Mol.Biol. 354 (2020) 1–61.
[25] Z. Li, A. Dai, M. Yang, S. Chen, Z. Deng, p38MAPK signaling pathway in osteoarthritis: pathological and therapeutic aspects, J. Inflamm. Res. 15 (2022) 723–734.
[26] Y. Zhang, T. Pizzute, M. Pei, A review of crosstalk between MAPK and Wnt signals and its impact on cartilage regeneration, Cell Tissue Res. 358 (2014) 633–649.
[27] C.K. Lee, R.G. Klopp, R. Weindruch, T.A. Prolla, Gene expression profile of aging and its retardation by caloric restriction, Science 285 (1999) 1390–1393.
[28] D.A. Bota, H. Van Remmen, K.J. Davies, Modulation of Lon protease activity and aconitase turnover during aging and oxidative stress, FEBS Lett. 532 (2002) 103–106.
[29] M. Pinti, L. Gibellini, Y. Liu, S. Xu, B. Lu, A. Cossarizza, Mitochondrial Lon protease at the crossroads of oxidative stress, ageing and cancer, Cell. Mol. Life Sci. 72 (2015) 4807–4824.
[30] A.V. Cordeiro, R.S. Brícola, R.R. Braga, L. Lenhare, V.R.R. Silva, C.P. Anaruma, E. R. Ropelle, et al., Aerobic exercise training induces the mitonuclear imbalance and UPRmt in the skeletal muscle of aged mice, J. Gerontol. A Biol. Sci. Med. Sci. 75 (2020) 2258–2261.
[31] L. Wang, Z. Feng, X. Wang, X. Wang, X. Zhang, DEGseq: an R package for identifying differentially expressed genes from RNA-seq data, Bioinformatics 26 (2010) 136–138.
[32] D. Szklarczyk, A. Franceschini, M. Kuhn, M. Simonovic, A. Roth, P. Minguez, C. von Mering, et al., The STRING database in 2011: functional interaction networks of proteins, globally integrated and scored, Nucleic Acids Res. 39 (2011) D561–D568.
[33] D. Szklarczyk, A.L. Gable, D. Lyon, A. Junge, S. Wyder, J. Huerta-Cepas, C. V. Mering, et al., STRING v11: protein-protein association networks with increased coverage, supporting functional discovery in genome-wide experimental datasets, Nucleic Acids Res. 47 (2019) D607–d613.
[34] P. Shannon, A. Markiel, O. Ozier, N.S. Baliga, J.T. Wang, D. Ramage, T. Ideker, et al., Cytoscape: a software environment for integrated models of biomolecular interaction networks, Genome Res. 13 (2003) 2498–2504.
[35] M.E. Smoot, K. Ono, J. Ruscheinski, P.L. Wang, T. Ideker, Cytoscape 2.8: new features for data integration and network visualization, Bioinformatics 27 (2011) 431–432.

[36] M. Ashburner, C.A. Ball, J.A. Blake, D. Botstein, H. Butler, J.M. Cherry, G. Sherlock, et al., Gene ontology: tool for the unification of biology. The Gene Ontology Consortium, Nat. Genet. 25 (2000) 25–29.
[37] M. Kanehisa, S. Goto, KEGG: kyoto encyclopedia of genes and genomes, Nucleic Acids Res. 28 (2000) 27–30.
[38] K.P. Pritzker, S. Gay, S.A. Jimenez, K. Ostergaard, J.P. Pelletier, P.A. Revell, W. B. van den Berg, et al., Osteoarthritis cartilage histopathology: grading and staging, Osteoarthritis Cartilage 14 (2006) 13–29.
[39] S.E. Calvo, K.R. Clauser, V.K. Mootha, MitoCarta2.0: an updated inventory of mammalian mitochondrial proteins, Nucleic Acids Res. 44 (2016) D1251–D1257.
[40] K. Szczepanowska, A. Trifunovic, Mitochondrial Matrix Proteases: Quality Control and beyond, FEBS J, 2021.
[41] D.L. Batiste, A. Kirkley, S. Laverty, L.M. Thain, A.R. Spouge, J.S. Gati, D. W. Holdsworth, et al., High-resolution MRI and micro-CT in an ex vivo rabbit anterior cruciate ligament transection model of osteoarthritis, Osteoarthritis Cartilage 12 (2004) 614–626.
[42] J. Nunnari, A. Suomalainen, Mitochondria: in sickness and in health, Cell 148 (2012) 1145–1159.
[43] C. Vazquez-Calvo, T. Suhm, S. Büttner, M. Ott, The basic machineries for mitochondrial protein quality control, Mitochondrion 50 (2020) 121–131.
[44] V. Eisner, M. Picard, G. Hajnóczky, Mitochondrial dynamics in adaptive and maladaptive cellular stress responses, Nat. Cell Biol. 20 (2018) 755–765.
[45] D.C. Chan, Fusion and fission: interlinked processes critical for mitochondrial health, Annu. Rev. Genet. 46 (2012) 265–287.
[46] R.J. Youle, A.M. van der Bliek, Mitochondrial fission, fusion, and stress, Science 337 (2012) 1062–1065.
[47] S.M. Jin, R.J. Youle, PINK1- and Parkin-mediated mitophagy at a glance, J. Cell Sci. 125 (2012) 795–799.
[48] D. Narendra, J.E. Walker, R. Youle, Mitochondrial quality control mediated by PINK1 and Parkin: links to parkinsonism, Cold Spring Harbor Perspect. Biol. 4 (2012).
[49] F. Randow, R.J. Youle, Self and nonself: how autophagy targets mitochondria and bacteria, Cell Host Microbe 15 (2014) 403–411.
[50] G. Jacquemin, D. Margiotta, A. Kasahara, E.Y. Bassoy, M. Walch, J. Thiery, D. Martinvalet, et al., Granzyme B-induced mitochondrial ROS are required for apoptosis, Cell Death Differ. 22 (2015) 862–874.
[51] L.A. Esposito, S. Melov, A. Panov, B.A. Cottrell, D.C. Wallace, Mitochondrial disease in mouse results in increased oxidative stress, Proc. Natl. Acad. Sci. U. S. A. 96 (1999) 4820–4825.
[52] W. Fan, C.S. Lin, P. Potluri, V. Procaccio, D.C. Wallace, mtDNA lineage analysis of mouse L-cell lines reveals the accumulation of multiple mtDNA mutants and intermolecular recombination, Genes Dev. 26 (2012) 384–394.
[53] E. Mirhadi, B.D. Roufogalis, M. Banach, M. Barati, A. Sahebkar, Resveratrol: mechanistic and therapeutic perspectives in pulmonary arterial hypertension, Pharmacol. Res. 163 (2021), 105287.
[54] L.H. Duntas, Resveratrol and its impact on aging and thyroid function, J. Endocrinol. Invest. 34 (2011) 788–792.
[55] H. Gu, K. Li, X. Li, X. Yu, W. Wang, L. Ding, L. Liu, Oral resveratrol prevents osteoarthritis progression in C57BL/6J mice fed a high-fat diet, Nutrients 8 (2016) 233.
[56] J.K. Ngo, K.J. Davies, Importance of the lon protease in mitochondrial maintenance and the significance of declining lon in aging, Ann. N. Y. Acad. Sci. 1119 (2007) 78–87.
[57] Z. Xu, T. Fu, Q. Guo, D. Zhou, W. Sun, Z. Zhou, Z. Gan, et al., Disuse-associated loss of the protease LONP1 in muscle impairs mitochondrial function and causes reduced skeletal muscle mass and strength, Nat. Commun. 13 (2022) 894.
[58] M.M. Temple, W.C. Bae, M.Q. Chen, M. Lotz, D. Amiel, R.D. Coutts, R.L. Sah, Age- and site-associated biomechanical weakening of human articular cartilage of the femoral condyle, Osteoarthritis Cartilage 15 (2007) 1042–1052.
[59] T. Wells, C. Davidson, M. Mörgelin, J.L. Bird, M.T. Bayliss, J. Dudhia, Age-related changes in the composition, the molecular stoichiometry and the stability of proteoglycan aggregates extracted from human articular cartilage, Biochem. J. 370 (2003) 69–79.
[60] Y.A. Rim, Y. Nam, J.H. Ju, The role of chondrocyte hypertrophy and senescence in osteoarthritis initiation and progression, Int. J. Mol. Sci. 21 (2020).
[61] T.F. Linsenmayer, B.P. Toole, R.L. Trelstad, Temporal and spatial transitions in collagen types during embryonic chick limb development, Dev. Biol. 35 (1973) 232–239.
[62] M.B. Mueller, R.S. Tuan, Functional characterization of hypertrophy in chondrogenesis of human mesenchymal stem cells, Arthritis Rheum. 58 (2008) 1377–1388.
[63] D. Studer, C. Millan, E. Öztürk, K. Maniura-Weber, M. Zenobi-Wong, Molecular and biophysical mechanisms regulating hypertrophic differentiation in chondrocytes and mesenchymal stem cells, Eur. Cell. Mater. 24 (2012) 118–135, discussion 135.
[64] W. Wu, R.C. Billinghurst, I. Pidoux, J. Antoniou, D. Zukor, M. Tanzer, A.R. Poole, Sites of collagenase cleavage and denaturation of type II collagen in aging and osteoarthritic articular cartilage and their relationship to the distribution of matrix metalloproteinase 1 and matrix metalloproteinase 13, Arthritis Rheum. 46 (2002) 2087–2094.
[65] A.P. Hollander, I. Pidoux, A. Reiner, C. Rorabeck, R. Bourne, A.R. Poole, Damage to type II collagen in aging and osteoarthritis starts at the articular surface, originates around chondrocytes, and extends into the cartilage with progressive degeneration, J. Clin. Invest. 96 (1995) 2859–2869.
[66] M. Aurich, A.R. Poole, A. Reiner, C. Mollenhauer, A. Margulis, K.E. Kuettner, A. A. Cole, Matrix homeostasis in aging normal human ankle cartilage, Arthritis Rheum. 46 (2002) 2903–2910.
[67] D. Parsch, T.H. Brümmendorf, W. Richter, J. Fellenberg, Replicative aging of human articular chondrocytes during ex vivo expansion, Arthritis Rheum. 46 (2002) 2911–2916.
[68] J.A. Martin, J.A. Buckwalter, Telomere erosion and senescence in human articular cartilage chondrocytes, J. Gerontol. A Biol. Sci. Med. Sci. 56 (2001) B172–B179.
[69] G.P. Dimri, X. Lee, G. Basile, M. Acosta, G. Scott, C. Roskelley, et al., A biomarker that identifies senescent human cells in culture and in aging skin in vivo, Proc. Natl. Acad. Sci. U. S. A. 92 (1995) 9363–9367.
[70] Y. Chen, Y. Yu, Y. Wen, J. Chen, J. Lin, Z. Sheng, H. Ouyang, et al., A high-resolution route map reveals distinct stages of chondrocyte dedifferentiation for cartilage regeneration, Bone Res 10 (38) (2022).
[71] J.S. Price, J.G. Waters, C. Darrah, C. Pennington, D.R. Edwards, S.T. Donell, I. M. Clark, The role of chondrocyte senescence in osteoarthritis, Aging Cell 1 (2002) 57–65.
[72] C. Fitzmaurice, C. Allen, R.M. Barber, L. Barregard, Z.A. Bhutta, H. Brenner, M. Naghavi, et al., Global, regional, and national cancer incidence, mortality, years of life lost, years lived with disability, and disability-adjusted life-years for 32 cancer groups, 1990 to 2015: a systematic analysis for the global burden of disease study, JAMA Oncol. 3 (2017) 524–548.
[73] Y. Wang, X. Zhao, M. Lotz, R. Terkeltaub, R. Liu-Bryan, Mitochondrial biogenesis is impaired in osteoarthritis chondrocytes but reversible via peroxisome proliferator-activated receptor γ coactivator 1α, Arthritis Rheumatol. 67 (2015) 2141–2153.
[74] J.A. Martin, J.A. Buckwalter, The role of chondrocyte senescence in the pathogenesis of osteoarthritis and in limiting cartilage repair, J. Bone Joint Surg. Am. 85 (A Suppl 2) (2003) 106–110.
[75] C. Vaamonde-García, R.R. Riveiro-Naveira, M.N. Valcárcel-Ares, L. Hermida-Carballo, F.J. Blanco, M.J. López-Armada, Mitochondrial dysfunction increases inflammatory responsiveness to cytokines in normal human chondrocytes, Arthritis Rheum. 64 (2012) 2927–2936.
[76] K.N. Reed, G. Wilson, A. Pearsall, V.I. Grishko, The role of mitochondrial reactive oxygen species in cartilage matrix destruction, Mol. Cell. Biochem. 397 (2014) 195–201.
[77] M.C. Coleman, J.E. Goetz, M.J. Brouillette, D. Seol, M.C. Willey, E.B. Petersen, J. A. Martin, et al., Targeting mitochondrial responses to intra-articular fracture to prevent posttraumatic osteoarthritis, Sci. Transl. Med. 10 (2018), eaan5372.
[78] B.M. Baker, C.M. Haynes, Mitochondrial protein quality control during biogenesis and aging, Trends Biochem. Sci. 36 (2011) 254–261.
[79] Y. Matsushima, L.S. Kaguni, Matrix proteases in mitochondrial DNA function, Biochim. Biophys. Acta 1819 (2012) 1080–1087.
[80] H.M. Ni, J.A. Williams, W.X. Ding, Mitochondrial dynamics and mitochondrial quality control, Redox Biol. 4 (2015) 6–13.
[81] O. Zurita Rendón, E.A. Shoubridge, LONP1 is required for maturation of a subset of mitochondrial proteins, and its loss elicits an integrated stress response, Mol. Cell Biol. 38 (2018).
[82] A.M. van der Bliek, Q. Shen, S. Kawajiri, Mechanisms of mitochondrial fission and fusion, Cold Spring Harbor Perspect. Biol. 5 (2013).
[83] S.M. Jin, R.J. Youle, The accumulation of misfolded proteins in the mitochondrial matrix is sensed by PINK1 to induce PARK2/Parkin-mediated mitophagy of polarized mitochondria, Autophagy 9 (2013) 1750–1757.
[84] X.M. Yin, W.X. Ding, The reciprocal roles of PARK2 and mitofusins in mitophagy and mitochondrial spheroid formation, Autophagy 9 (2013) 1687–1692.
[85] P.M. Quirós, Y. Español, R. Acín-Pérez, F. Rodríguez, C. Bárcena, K. Watanabe, C. López-Otín, et al., ATP-dependent Lon protease controls tumor bioenergetics by reprogramming mitochondrial activity, Cell Rep. 8 (2014) 542–556.
[86] K.R. Pryde, J.W. Taanman, A.H. Schapira, A LON-ClpP proteolytic Axis degrades complex I to extinguish ROS production in depolarized mitochondria, Cell Rep. 17 (2016) 2522–2531.
[87] E.L. Robb, A.R. Hall, T.A. Prime, S. Eaton, M. Szibor, C. Viscomi, M.P. Murphy, et al., Control of mitochondrial superoxide production by reverse electron transport at complex I, J. Biol. Chem. 293 (2018) 9869–9879.
[88] S. Verkaart, W.J. Koopman, S.E. van Emst-de Vries, L.G. Nijtmans, L.W. van den Heuvel, J.A. Smeitink, P.H. Willems, Superoxide production is inversely related to complex I activity in inherited complex I deficiency, Biochim. Biophys. Acta 1772 (2007) 373–381.
[89] I. Dolado, A. Swat, N. Ajenjo, G. De Vita, A. Cuadrado, A.R. Nebreda, p38alpha MAP kinase as a sensor of reactive oxygen species in tumorigenesis, Cancer Cell 11 (2007) 191–205.
[90] P. Santabárbara-Ruiz, M. López-Santillán, I. Martínez-Rodríguez, A. Binagui-Casas, L. Pérez, M. Milán, F. Serras, et al., ROS-induced JNK and p38 signaling is required for unpaired cytokine activation during Drosophila regeneration, PLoS Genet. 11 (2015), e1005595.
[91] I. Rego-Pérez, A. Durán-Sotuela, P. Ramos-Louro, F.J. Blanco, Mitochondrial genetics and epigenetics in osteoarthritis, Front. Genet. 10 (2019) 1335.
[92] Q. Zhao, J. Wang, I.V. Levichkin, S. Stasinopoulos, M.T. Ryan, N.J. Hoogenraad, A mitochondrial specific stress response in mammalian cells, EMBO J. 21 (2002) 4411–4419.
[93] C. Münch, J.W. Harper, Mitochondrial unfolded protein response controls matrix pre-RNA processing and translation, Nature 534 (2016) 710–713.
[94] L. Vidal-Bralo, Y. Lopez-Golan, A. Mera-Varela, I. Rego-Perez, S. Horvath, Y. Zhang, A. Gonzalez, et al., Specific premature epigenetic aging of cartilage in osteoarthritis, Aging (Albany NY) 8 (2016) 2222–2231.
[95] M. Zhang, J.L. Theleman, K.A. Lygrisse, J. Wang, Epigenetic mechanisms underlying the aging of articular cartilage and osteoarthritis, Gerontology 65 (2019) 387–396.